



# University of HUDDERSFIELD

## University of Huddersfield Repository

Dhimish, Mahmoud, Holmes, Violeta, Mehrdadi, Bruce and Dales, Mark

Comparing Mamdani Sugeno fuzzy logic and RBF ANN network for PV fault detection

### Original Citation

Dhimish, Mahmoud, Holmes, Violeta, Mehrdadi, Bruce and Dales, Mark (2018) Comparing Mamdani Sugeno fuzzy logic and RBF ANN network for PV fault detection. *Renewable Energy*, 117. pp. 257-274. ISSN 0960-1481

This version is available at <http://eprints.hud.ac.uk/id/eprint/33780/>

The University Repository is a digital collection of the research output of the University, available on Open Access. Copyright and Moral Rights for the items on this site are retained by the individual author and/or other copyright owners. Users may access full items free of charge; copies of full text items generally can be reproduced, displayed or performed and given to third parties in any format or medium for personal research or study, educational or not-for-profit purposes without prior permission or charge, provided:

- The authors, title and full bibliographic details is credited in any copy;
- A hyperlink and/or URL is included for the original metadata page; and
- The content is not changed in any way.

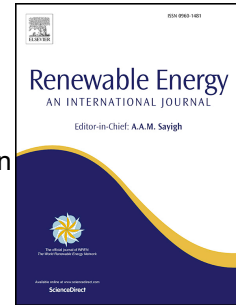
For more information, including our policy and submission procedure, please contact the Repository Team at: [E.mailbox@hud.ac.uk](mailto:E.mailbox@hud.ac.uk).

<http://eprints.hud.ac.uk/>

# Accepted Manuscript

Comparing Mamdani Sugeno fuzzy logic and RBF ANN network for PV fault detection

Mahmoud Dhimish, Violeta Holmes, Bruce Mehrdadi, Mark Dales



PII: S0960-1481(17)31027-3

DOI: [10.1016/j.renene.2017.10.066](https://doi.org/10.1016/j.renene.2017.10.066)

Reference: RENE 9354

To appear in: *Renewable Energy*

Received Date: 4 May 2017

Revised Date: 27 August 2017

Accepted Date: 23 October 2017

Please cite this article as: Dhimish M, Holmes V, Mehrdadi B, Dales M, Comparing Mamdani Sugeno fuzzy logic and RBF ANN network for PV fault detection, *Renewable Energy* (2017), doi: 10.1016/j.renene.2017.10.066.

This is a PDF file of an unedited manuscript that has been accepted for publication. As a service to our customers we are providing this early version of the manuscript. The manuscript will undergo copyediting, typesetting, and review of the resulting proof before it is published in its final form. Please note that during the production process errors may be discovered which could affect the content, and all legal disclaimers that apply to the journal pertain.

# Comparing Mamdani Sugeno Fuzzy Logic and RBF ANN Network for PV Fault Detection

Mahmoud Dhimish, Violeta Holmes, Bruce Mehrdadi, Mark Dales

School of Computing and Engineering, University of Huddersfield, United Kingdom

---

## **Abstract**

This work proposes a new fault detection algorithm for photovoltaic (PV) systems based on artificial neural networks (ANN) and fuzzy logic system interface. There are few instances of machine learning techniques deployed in fault detection algorithms in PV systems, therefore, the main focus of this paper is to create a system capable to detect possible faults in PV systems using radial basis function (RBF) ANN network and both Mamdani, Sugeno fuzzy logic systems interface.

The obtained results indicate that the fault detection algorithm can detect and locate accurately different types of faults such as, faulty PV module, two faulty PV modules and partial shading conditions affecting the PV system. In order to achieve high rate of detection accuracy, four various ANN networks have been tested. The maximum detection accuracy is equal to 92.1%. Furthermore, both examined fuzzy logic systems show approximately the same output during the experiments. However, there are slightly difference in developing each type of the fuzzy systems such as the output membership functions and the rules applied for detecting the type of the fault occurring in the PV plant.

**Keywords:** *Photovoltaic System, Photovoltaic Faults, Fault Detection, ANN Networks, Fuzzy Logic Systems*

---

## **1. INTRODUCTION**

The monitoring and regular performance supervision on the functioning of grid-connected photovoltaic (GCPV) systems is necessary to ensure an optimal energy harvesting and reliable power production. The development of diagnostic methods for fault detection in the PV systems behaviour is particularly important due to the expansion degree of GCPV systems nowadays and the need to optimize their reliability and performance.

There are existing techniques which were developed for possible fault detection in grid-connected PV systems. Some of these techniques use meteorological and satellite data for predicting the faults in the GCPV plants [1 & 2]. However, some of the PV fault detecting algorithms do not require any climate data (solar irradiance and module temperature) such as the earth capacitance measurements established by Taka-Shima [3].

Other PV fault detection algorithms is based on the comparison of simulated and measured yield by analysing the losses of the DC side of the GCPV plant [4-6]. Furthermore, a fault detection method based on the ratio of DC side and the AC side of the PV system is proposed by W. Chine et al [7]. The method can detect five different faults such as faulty modules in a PV string, faulty DC/AC inverter and faulty maximum power point tracking (MPPT) units. On the other hand, S. Silvestre et al [8] proposed a new procedure for fault detection in GCPV systems based on the evaluation of the current and the voltage

40 indicators. The main advantage of this algorithm is to reduce the number of monitoring sensors in the PV  
41 plants and integrating a fault detection algorithm into an inverter without using simulation software or  
42 additional external hardware devices.

43 Further fault detection algorithms focus on faults occurring in the AC-side of GCPV systems, as proposed  
44 by M. Dhimish et al [9]. The approach uses mathematical analysis technique for identifying faulty  
45 conditions in the DC/AC inverter units. Moreover, hot-spot detection in PV substrings using the AC  
46 parameters characterization was developed by [10]. The hot-spot detection method can be further used  
47 and integrated with DC/DC power converters that operates at the subpanel level. A comprehensive review  
48 of the faults, trends and challenges of the grid-connected PV systems is shown in [11-13].

49 Other PV fault detection approaches use statistical analysis techniques for identifying micro cracks and  
50 their impact of the PV output power as presented by [14]. However, T. Zhao at al [15] developed a  
51 decision tree (DT) technique for examining two different types of fault using an over-current protection  
52 device (OVPD). The first type of fault is the line-to-line that occurs under low irradiance conditions, and  
53 the second is line-to-line faults occurring in PV arrays equipped with blocking diodes.

54 PV systems reliability improvement by real-time field programmable gate array (FPGA) based on switch  
55 failures diagnosis and fault tolerant DC-DC converters is presented by [16]. B. Chong [17] suggested a  
56 controller design for integrated PV converter modules under partial shading conditions. The developed  
57 approach is based on a novel model-based, two-loop control scheme for a particular MIPC system, where  
58 bidirectional Cuk DC-DC converters are used as the bypass converters and a terminal Cuk boost  
59 functioning as a while system power conditioner.

60 Nowadays, fuzzy logic systems widely used with GCPV plants. R. Boukenoui et al [18] proposed a new  
61 intelligent MPPT method for standalone PV system operating under fast transient variations based on  
62 fuzzy logic controller (FLC) with scanning and storing algorithm. Furthermore, [19] presents an adaptive  
63 FLC design technique for PV inverters using differential search algorithm. Furthermore, N. Sa-ngawong  
64 & I. Ngamroo [20] proposed an intelligent PV farms for robust frequency stabilization in multi-area  
65 interconnected power systems using Sugeno fuzzy logic control, similar approach was developed by [21]  
66 for power optimization in standalone PV systems.

67 In [22 & 23] authors have used a Mamdani fuzzy logic classification system which consists of two inputs,  
68 the voltage and power ratio, and one output membership function. The results can accurately detect  
69 several faults in the PV system such as partial shading and short circuited PV modules.

70 Artificial intelligent networks (ANN) is another machine leaning technique nowadays is used for  
71 detecting faults in PV systems. A learning method based on expert systems is developed by [24] to  
72 identify two types of fault (due to the shading effect and to the inverter's failure). Whereas [25] proposed  
73 an ANN network that detects faults in the DC side of PV systems which includes faulty bypass diodes  
74 and faulty PV modules in a PV string.

75 A. Millit et al [26] shows that ANN networks is a possible solution for modelling and estimating the  
76 output power of a GCPV systems. However, a failure mode prediction and energy harvesting of PV plants  
77 to assist dynamic maintenance tasks using ANN based models is proposed by F. Polo et al [27]. Further  
78 investigation on a very short term load forecasting for a distribution system with high PV penetration is  
79 suggested by S. Sepasi [28]. Finally, B. Amrouche & X. Pivert [30] offered an ANN network based daily  
80 local forecasting for global solar radiation (GHI). The ANN model is developed to predict the local GHI  
81 based on a daily weather forecast provided by the US National Oceanic and Atmospheric Administration  
82 (NOAA) for four neighbouring locations.

83 The main contribution of this work is to present a new algorithm for isolation and identification of the  
 84 faults accruing in a PV system. The algorithm is capable to detect several faults such as faulty PV module  
 85 in a PV string, faulty PV string, faulty MPPT, and partial shading conditions effects the PV system. The  
 86 proposed algorithm is comparing between two different approaches for detecting failure conditions which  
 87 can be described as the following:

- 88 1. Artificial Neural Network (ANN) Approach:  
 89 Four different ANN networks have been compared using a logged data of several faulty  
 90 conditions affecting the examined PV plant. The maximum PV fault detection accuracy achieved  
 91 by the ANN networks is equal to 92.1%.  
 92
- 93 2. Fuzzy Logic Fault Classification Approach:  
 94 This approach consists of two types of fuzzy logic interface systems: Mamdani and Sugeno. Both  
 95 fuzzy interface systems were briefly compared and developed using MATLAB/Simulink  
 96 software. This approach was tested using a faulty PV data which was logged from the examined  
 97 1.1 kWp PV plant installed at the University of Huddersfield.

98 The overall system design is shown in Fig. 1. The PV plant has a capacity of 1.1 kWp. A computer  
 99 interface has two options, a PV fault detection algorithms which use MATLAB/Simulink software which  
 100 contains the ANN and the fuzzy logic interface system. Furthermore, LabVIEW software is used for the  
 101 real-time long-term data monitoring as well as, data logging software environment.

102 This paper is organized as follows: Section 2 presents the data acquisition in the PV plant. Section 3  
 103 describes the methodology used, Fault detection algorithm and diagnosis rules are presented, while  
 104 section 4 lists the results and discussion of the work. Finally, section 5 describes the conclusion and future

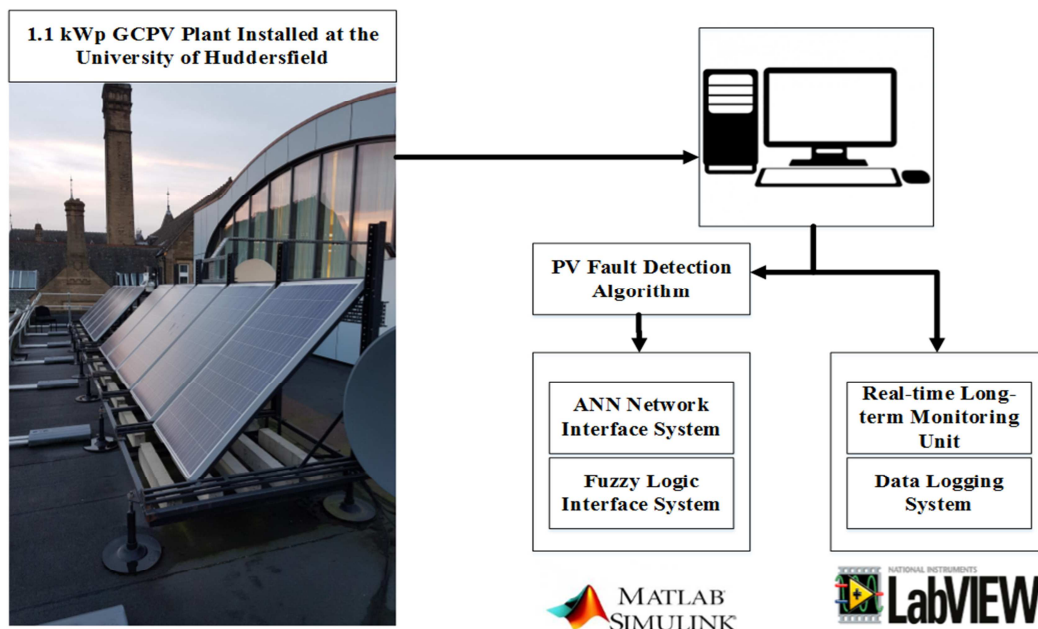


Fig. 1. Overall System Architecture Design for the Examined PV Plant

105 work.

## 106 2. *Faults in Photovoltaic Plants*

107 The faults occurring in a PV system are mainly related to the PV array, MPPT units, DC/AC inverters, the  
 108 storage system and the electrical grid. This work aims to detecting the faults occurring in the PV array  
 109 and, with reference to Table 1, eleven different fault are investigated.

110 It is worthy to mention that PS conditions used in this work corresponds to an irradiance level affects all

TABLE 1  
DIFFERENT TYPE OF FAULTS OCCURRING IN THE EXAMINED PV PLANT

Type of Fault	Symbol
Normal Operation and PS effects the PV system	F1
One faulty PV module	F2
Two faulty PV modules	F3
Three faulty PV modules	F4
Four faulty PV modules	F5
One faulty PV module and PS effects the PV system	F6
Two faulty PV modules and PS effects the PV system	F7
Three faulty PV modules and PS effects the PV system	F8
Four faulty PV modules and PS effects the PV system	F9
Faulty PV String	F10
Faulty MPPT unit	F11

111 examined PV modules. Thus, during the experiments, all examined PV modules were tested under the  
 112 same PS conditions with different shading percentages (20%, 30%, etc.).

## 113 3. *METHODOLOGY*

114 This section reports the PV data acquisition system, PV theoretical modelling, the overall fault detection  
 115 algorithm, and the detailed design of the proposed artificial neural network and the fuzzy logic interface  
 116 system.

### 117 3.1 *PV Plant and data Acquisition*

118 The PV system used in this work consists of a grid-connected PV plant comprising 5 polycrystalline  
 119 silicon PV modules each with a nominal power of 220 Wp. The photovoltaic modules are connected in  
 120 series. The photovoltaic string is connected to a Maximum Power Point Tracker (MPPT) with an output  
 121 efficiency of not less than 95.0% [31 & 32]. The DC current and voltage are measured using the internal  
 122 sensors which are part of the Flexmax MPPT unit.

123 A Vantage Pro monitoring unit is used to receive the Global solar irradiance measured by the Davis  
 124 weather station which includes a pyranometer. A Hub 4 communication manager is used to facilitate  
 125 acquisition of modules' temperature using the Davis external temperature sensor, and the electrical data  
 126 for each photovoltaic string. VI LabVIEW software is used to implement data logging and monitoring  
 127 functions of the PV system. Fig. 2 illustrates the overall system architecture of the PV plant.

128 The real-time measurements are taken by averaging 60 samples, gathered at a rate of 1 Hz over a period  
 129 of one minute. Therefore, the obtained results for power, voltage and current are calculated at one minute  
 130 intervals.

TABLE 2  
ELECTRICAL CHARACTERISTICS OF SMT6 (60) P PV MODULE

Solar Panel Electrical Characteristics	Value
Peak Power	220 W
Voltage at maximum power point ( $V_{mp}$ )	28.7 V
Current at maximum power point ( $I_{mp}$ )	7.67 A
Open Circuit Voltage ( $V_{OC}$ )	36.74 V
Short Circuit Current ( $I_{sc}$ )	8.24 A
Number of cells connected in series	60
Number of cells connected in parallel	1
$R_s$ , $R_{sh}$	0.53 Ohms , 1890 Ohms
dark saturation current ( $I_o$ )	$2.8 \times 10^{-10}$ A
Ideal diode factor (A)	1.5
Boltzmann's constant (K)	$1.3806 \times 10^{-23}$ J.K <sup>-1</sup>

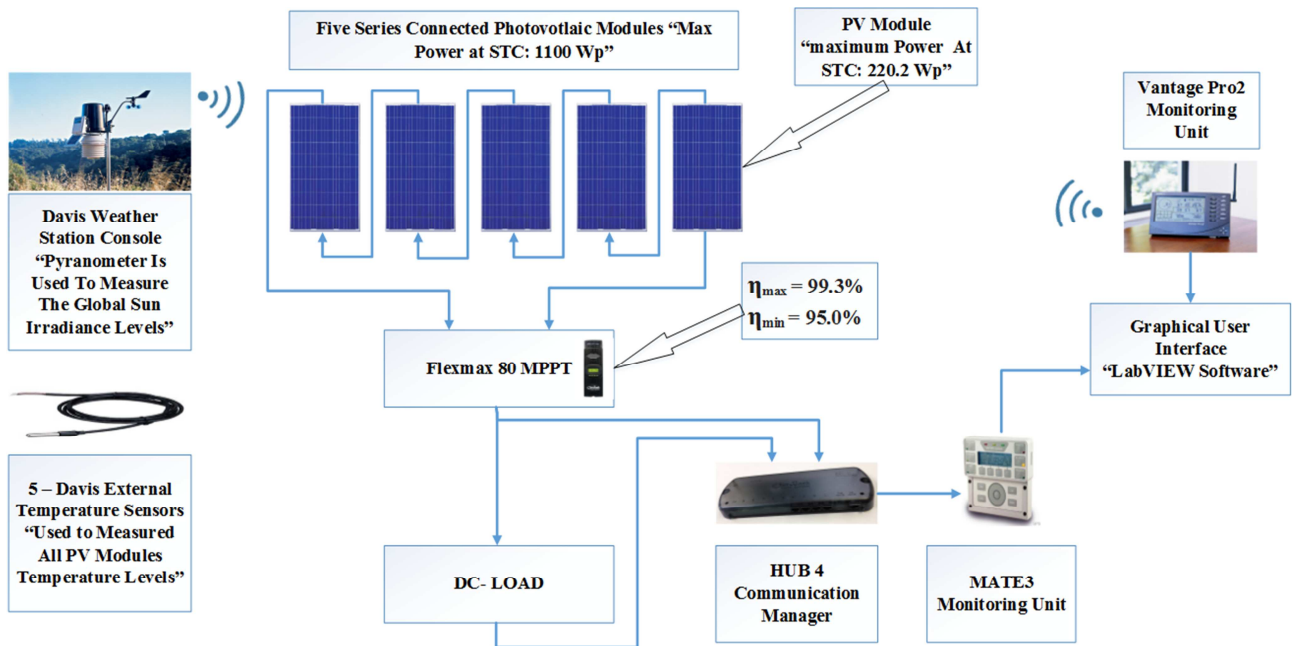


Fig. 2. Examined PV System Installed at the Huddersfield University, United Kingdom

131 The SMT6 (60) P solar module manufactured by Romag, has been used in this work. The electrical  
 132 characteristics of the solar module are shown in Table 2. The standard test condition (STC) for these solar  
 133 panels are: solar irradiance =  $1000 \text{ W/m}^2$ , module temperature =  $25 \text{ }^\circ\text{C}$

### 134 3.2. Photovoltaic Theoretical Modelling

135 The DC side of the PV system is modelled using the 5-parameter model. The voltage and current  
 136 characteristics of the PV module can be obtained using the single diode model [29] as follows:

$$137 \quad I = I_{ph} - I_0 \left( e^{\frac{V+IR_s}{N_s V_t}} - 1 \right) - \left( \frac{V+IR_s}{R_{sh}} \right) \quad (1)$$

138 where  $I_{ph}$  is the photo-generated current at STC,  $I_0$  is the dark saturation current at STC,  $R_s$  is the  
 139 module series resistance,  $R_{sh}$  is the panel parallel resistance,  $N_s$  is the number of series cells in the PV  
 140 module and  $V_t$  is the thermal voltage and it can be defined based on:

$$141 \quad V_t = \frac{A k T}{q} \quad (2)$$

142 where  $A$  the ideal diode factor,  $k$  is Boltzmann's constant and  $q$  is the charge of the electron.

143 The five parameter model is determined by solving the transcendental equation (1) using Newton-  
 144 Raphson algorithm [30] based only on the datasheet of the available parameters for the examined PV  
 145 module that was used in this work as shown in Table 1. The power produced by the PV module in watts  
 146 can be easily calculated along with the current (I) and voltage (V) that is generated by equation (1),  
 147 therefore:

$$148 \quad P_{\text{theoretical}} = I \times V \quad (3)$$

149 The Current-Voltage (I-V) and Power-Voltage (P-V) curves of the examined PV module is shown in Fig.  
 150 3(A) and Fig. 3(B) respectively. Three different simulation results is explained at 1000, 500, and 100  
 151  $\text{W/m}^2$ . However, the simulation temperature remains at STC (25 °C).

152 The purpose of using the analysis for the I-V and P-V curves, is to generate the expected output power of  
 153 the examined PV module, therefore, it can be used to predict the error between the real-time long-term  
 154 PV measured data and the theoretical power and voltage performance.

### 155 3.3 Overall PV Fault Detection Algorithm

156 In order to determine the type of a fault occurred in our PV plant, two ratios have been identified. Power  
 157 ratio (PR) and voltage ratio (VR) have been used to categorise the region of the fault because both ratios  
 158 have the following features:

- 159 1) Both ratios are changeable during faulty conditions in the PV system
- 160 2) When the power ratio is equal to zero, the voltage ratio can still have a value regarding the  
 161 voltage open circuit of the PV modules

162 The power and voltage ratios are given by the following expressions:

$$163 \quad PR = \frac{P_{\text{theoretical}}}{P_{\text{measured}}} \quad (4)$$

$$164 \quad VR = \frac{V_{\text{theoretical}}}{V_{\text{measured}}} \quad (5)$$

165 where  $P_{\text{theoretical}}$  is the theoretical output power generated by the PV system,  $P_{\text{measured}}$  is the measured  
 167

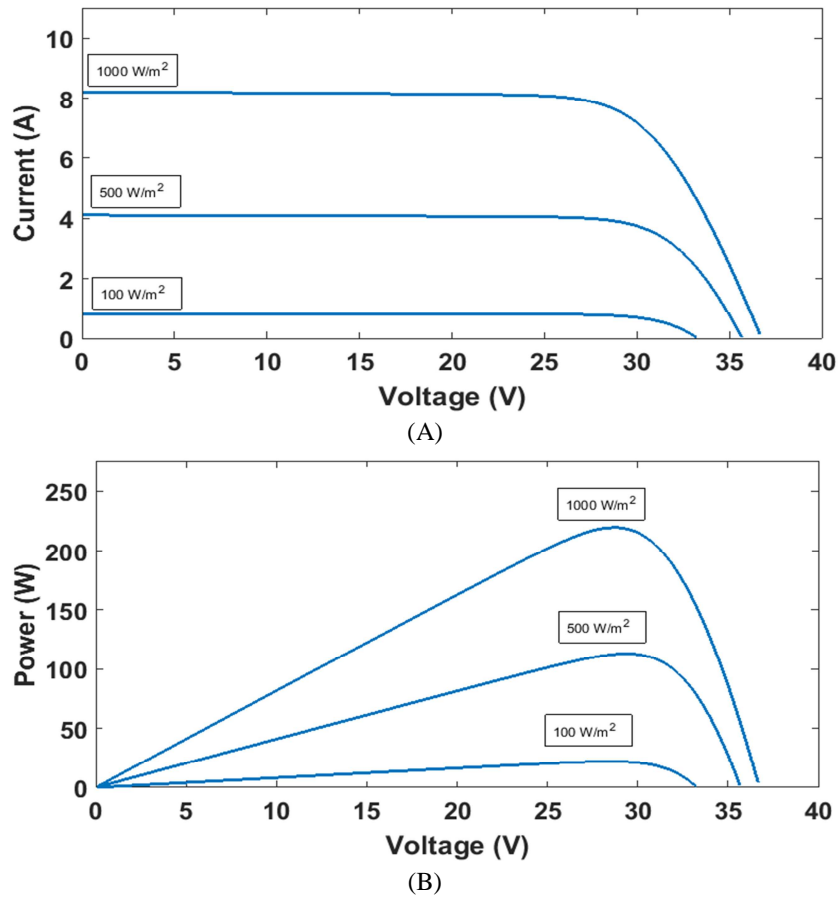


Fig. 3. Photovoltaic Theoretical Curves Modelling. (A) I-V Curve. (B) P-V Curve

168 output power from PV string,  $V_{theoretical}$  is the theoretical output voltage generated by the PV system  
 169 and  $V_{measured}$  is the measured output DC voltage from PV string.

170 Since the internal sensors of the MPPT have a conversion error rate of 95% as shown in Fig. 2, the power  
 171 ratios are calculated at 5% error tolerance of the theoretical power which presents the maximum error  
 172 condition for the examined PV system. Therefore, the maximum and minimum power and voltage ratios  
 173 are expressed by the following formulas which contains the tolerance rate of the MPPT units and the total  
 174 number of PV modules in the PV string:

$$175 \quad PR \min = \frac{P_{theoretical}}{P_{measured}} \quad (6)$$

$$176 \quad PR \max = \frac{P_{theoretical}}{P_{measured} \times MPPT \text{ Tolerance Rate}} \quad (7)$$

$$179 \quad VR \min = \frac{V_{theoretical}}{V_{measured}} \quad (8)$$

$$181 \quad VR \max = \frac{V_{theoretical}}{V_{measured} \times MPPT \text{ Tolerance Rate}} \quad (9)$$

184 The normal operation mode region of the examined PV plant at STC is shown in Fig. 4 case1, the values  
 185 of the PR can be calculated using (6 & 7) as the following:

$$186 \quad \text{Normal Operation Mode - PR min} = \frac{P_{theoretical}}{P_{measured}} = \frac{1100}{1100} = 1$$

$$187 \quad \text{Normal Operation Mode - PR max} = \frac{P_{theoretical}}{P_{measured} \times MPPT \text{ Tolerance Rate}} = \frac{1100}{1100 \times 95\%} = 1.053$$

188 As can be noticed from Fig. 4 case 2, the maximum partial shading condition detected by the irradiance  
 189 sensor is equal to 97.3%, therefore, the maximum PR is calculated as the following:

$$\text{Fault Detection Algorithm Maximum PR} = \frac{P_{theoretical}}{P_{measured} \times MPPT \text{ Tolerance Rate}} = \frac{1100}{23.66 \times 95\%} \approx 50$$

190 The value of the maximum PR is important because if the PR is greater than 50, then the fault detection  
 191 algorithm can specify whether a fault occurred in the MPPT unit or there is a complete disconnection of a  
 192 PV string from the entire PV system. In order to detect which type of fault accrued in the region of  $PR >$   
 193 50. The value of the voltage ratio has been considered, two conditions is selected:

- 194 1. If  $VR \geq 0$ , then a faulty PV string is detected
- 195 2. If  $VR = 0$ , then a faulty MPPT unit is detected

196 Furthermore, if the value of the PR does not lie within the normal operation mode region and it is not  
 197 higher than the PR max threshold ( $PR \geq 50$ ), then the value of the PR and VR is passed to the second part  
 198 of the fault detection algorithm which consists of two different machine learning techniques as shown in  
 199 Fig. 5.

200 The first technique is the artificial neural network (ANN). In order to select the most suitable ANN model  
 201 structure, four different ANN models have been developed:

- 202       • 2 Inputs, 5 outputs using 1 hidden layers  
 203       • 2 Inputs, 5 outputs using 2 hidden layers  
 204       • 2 Inputs, 9 outputs using 1 hidden layers  
 205       • 2 Inputs, 9 outputs using 2 hidden layers

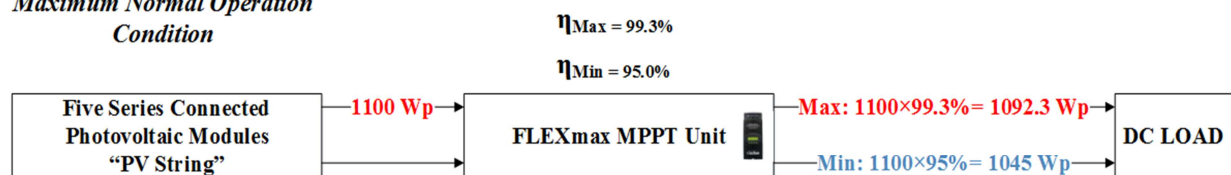
206 A brief illustration on the selection of the variables and ANN model structure is covered in the next  
 207 section (section 3.4).

208 The second machine learning technique used to detect possible faults occurring in the PV system is the  
 209 fuzzy logic. In this paper, two different fuzzy logic systems have been implemented:

- 210       • Mamdani-type fuzzy logic system interface  
 211       • Sugeno-type fuzzy logic system interface

212 The fuzzy logic systems are explained in section 3.5. Moreover, the type of the fault which can be  
 213 detected using the machine learning techniques are shown in Table 1.

***CASE1:***  
***Maximum Normal Operation***  
***Condition***



***CASE2:***  
***Maximum Partial Shading***  
***Condition (97.3%)***

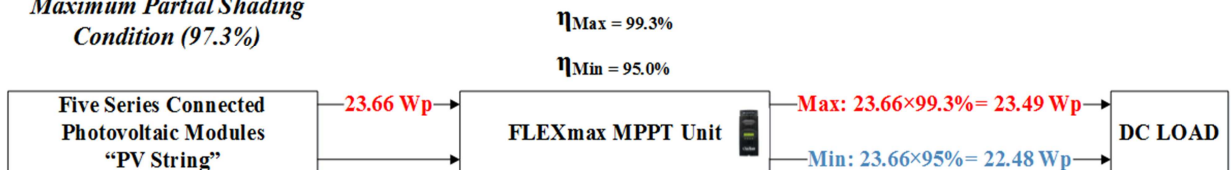


Fig. 4. DC side Numerical Calculations at Maximum and Minimum Operating Points

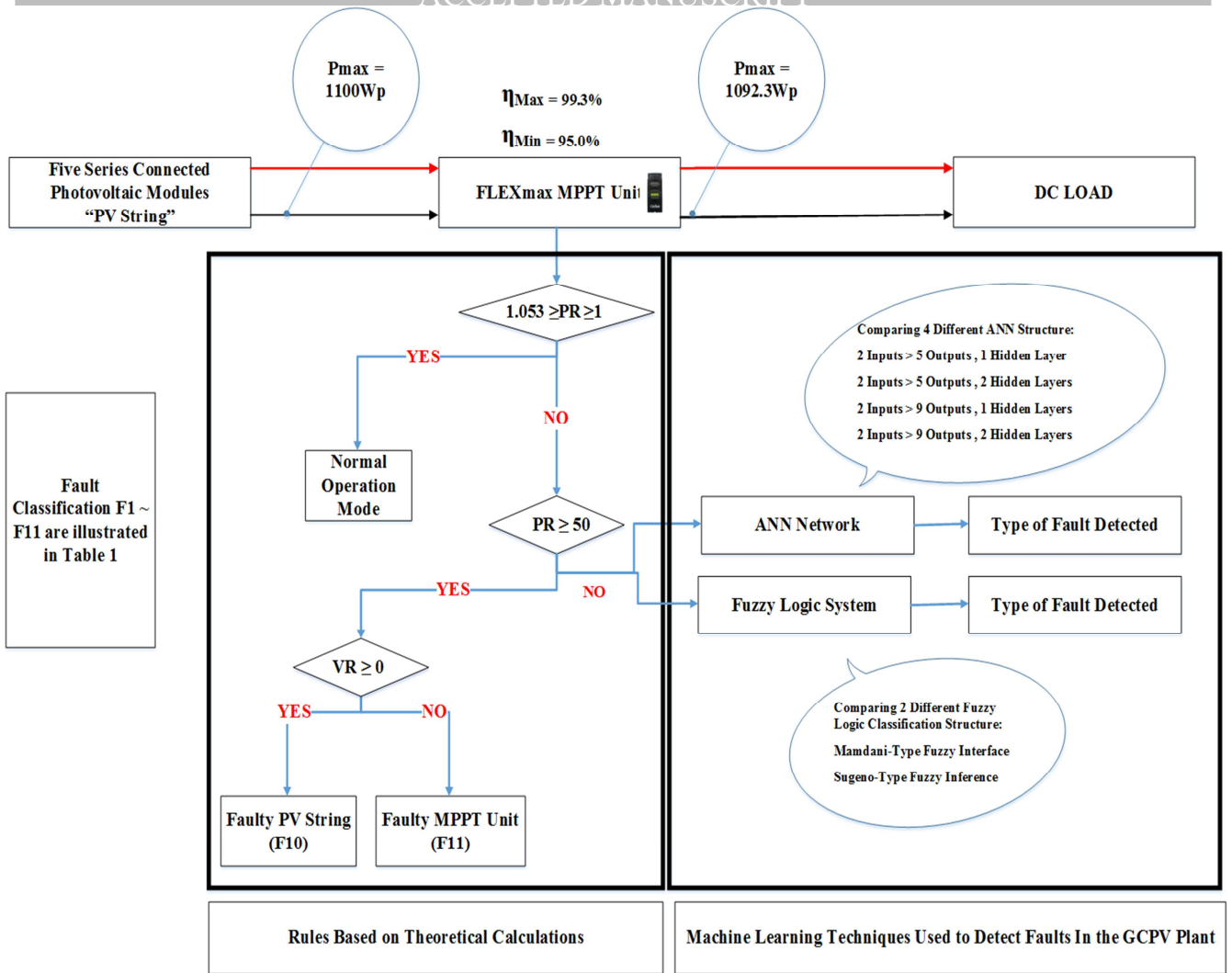


Fig. 5. Detailed PV Fault Detection Approach

### 214 3.4 ANN Model Implementation

215 The main objective of the ANN model is to detect possible faults in the examined PV system shown in  
 216 Fig. 2. The ANN model has been developed as follows:

- 217 • Selection of input and output variables
- 218 • Data set normalization
- 219 • Selection of network structure
- 220 • Network training
- 221 • Network test

222 The input parameters used to configure all tested ANN models are the VR and PR ratios which can be  
 223 calculated using (8 & 9) respectively. The Data set (input variables) are normalized within the range of -1  
 224 and +1 using (10).

$$225 \quad y = \frac{(y_{\max} - y_{\min})(x - x_{\min})}{(x_{\max} - x_{\min})} + y_{\min}$$

226 (10)

227 where  $x \in \{x_{min}, x_{max}\}$ ,  $y \in \{y_{min}, y_{max}\}$  and  $x$  is the original data value and  $y$  is the corresponding  
 228 normalized value with  $y_{min} = -1$  and  $y_{max} = +1$ .

229 In order to select the most efficient architecture for the ANN model, a comparison between four different  
 230 ANN models have been performed where the structure of all tested ANN networks is the Radial Basis  
 231 Function (RBF) as shown in Fig. 6.

232 ANN models A and B are using 2 inputs (VR & PR) and five outputs, where the hidden layers are equal  
 233 to one and two respectively. The purpose of increasing the hidden layers, is to increase the computational  
 234 performance of the ANN network, thus, increasing the detection accuracy (DA) of the ANN model. The  
 235 faults which can be detected using both ANN models are:

- 236 • F1: Partial Shading (PS) affecting the PV system
- 237 • F2: One faulty PV Module and PS affecting the PV system
- 238 • F3: Two faulty PV Modules and PS affecting the PV system
- 239 • F4: Three faulty PV Modules and PS affecting the PV system
- 240 • F5: Four faulty PV Modules and PS affecting the PV system

241 From the research conducted using several days measurements (briefly described in the results section),  
 242 the comparison between model A and model B shows that both models have a low detection accuracy  
 243 where the maximum achieved detection accuracy is equal to 77.7%. Therefore, this challenge was solved  
 244 by adding new types of faults for the ANN network that allows the ANN model to detect faulty PV  
 245 modules only (No PS on the entire PV plant).

246 ANN models C and D are using 2 inputs (VR & PR) and nine outputs, where the hidden layers are equal  
 247 to one and two respectively. The faults which can be detected using both ANN models are:

- 248 • F1: PS affecting the PV system
- 249 • F2: One faulty PV Module only
- 250 • F3: Two faulty PV Modules only
- 251 • F4: Three faulty PV Modules only
- 252 • F5: Four faulty PV modules only
- 253 • F6: One faulty PV Module and PS affecting the PV system
- 254 • F7: Two faulty PV Modules and PS affecting the PV system
- 255 • F8: Three faulty PV Modules and PS affecting the PV system
- 256 • F9: Four faulty PV Modules and PS affecting the PV system

257 In this study, the data set have been recorded from the experimental setup shown in Fig. 2. The data set  
 258 used to train, validate, and test the ANN networks contains 6480 measurements logged in 9 days as  
 259 shown in Fig. 7, where each day consists of 720 sample. During the experiment, the PV modules'  
 260 temperature is between 15.3 – 16.7 °C, the value of the VR and PR have been logged. Each day has a  
 261 different fault applied to the PV systems which can be simplified by the following:

- 262 • Day 1: Partial shading conditions affecting the PV system
- 263 • Day 2: One PV module has been disconnected from the PV system (faulty PV modules)
- 264 • Day 3: Two PV modules have been disconnected from the PV system
- 265 • Day 4: Three PV modules have been disconnected from the PV system
- 266 • Day 5: Four PV modules have been disconnected from the PV system
- 267 • Day 6: One PV module has been disconnected and PS applied to all other PV modules

- 268 • Day 7: Two PV modules have been disconnected and PS applied to all other PV modules
- 269 • Day 8: Three PV modules have been disconnected and PS applied to all other PV modules
- 270 • Day 9: Four PV modules have been disconnected and PS applied to all only existing PV module

271 The obtained measurements is then divided into three subsets:

- 272 1. 70% of the data are used to train the ANN networks.
- 273 2. 10% of samples are used to validate the ANN network. This test is not used in the training
- 274 process.
- 275 3. 20% of samples are used to test the actual ANN network detection accuracy.

276 The implementation of the ANN network has been developed using MATLAB/Simulink software. ALL  
 277 results obtained from the ANN network is discussed briefly in the results section, where the maximum  
 278 obtained detection accuracy among all tested ANN models is equal to 92.1% for the ANN model which  
 279 contains 2 inputs, 9 outputs using 2 hidden layers. Moreover, the minimum Mean Square Errors (MSE)  
 280 achieved during the training and test processes are 0.005 and 0.007 respectively.

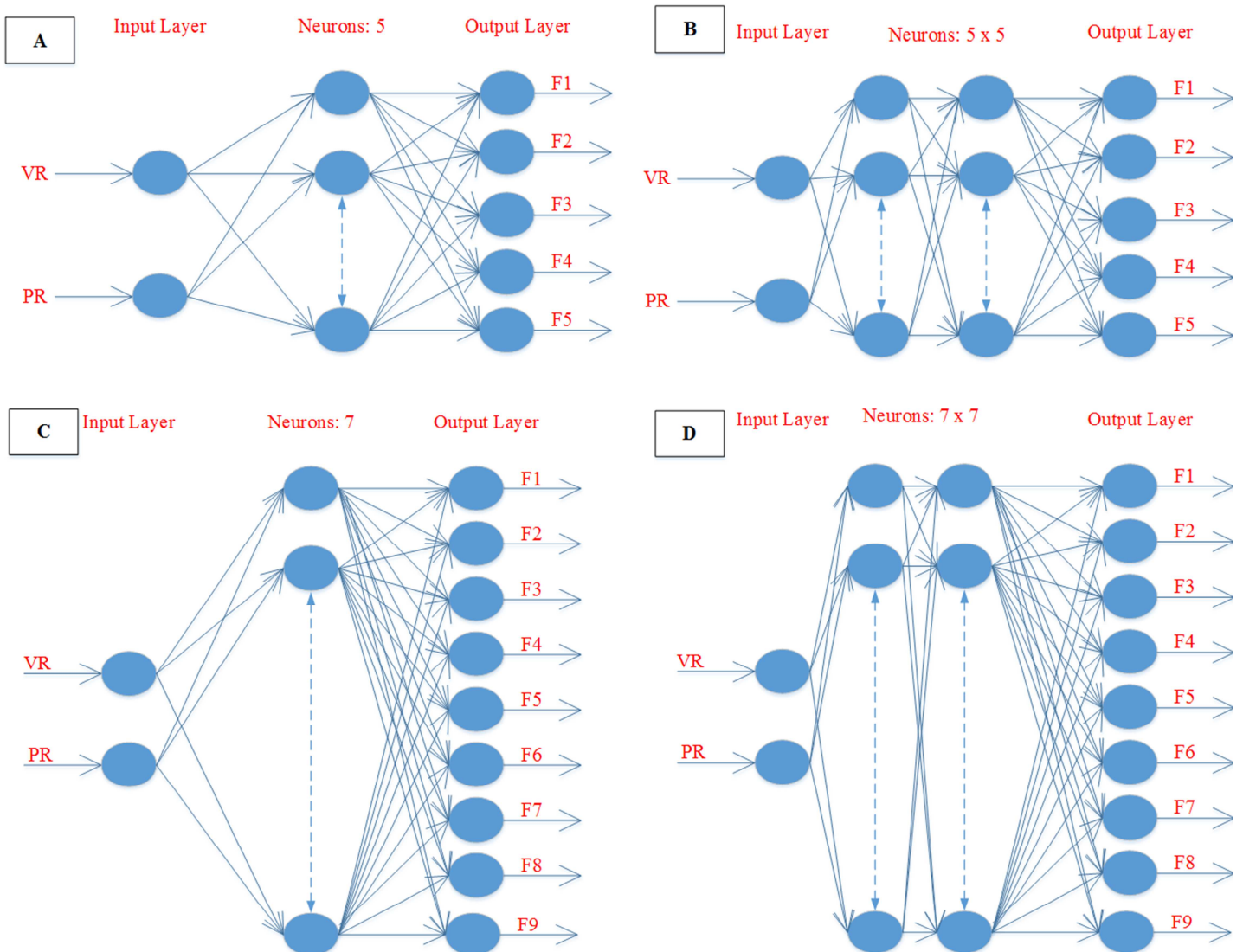


Fig. 6. The Adopted ANN Network. (A) 2 Inputs, 5 Outputs using 1 Hidden Layer, (B) 2 Inputs, 5 Outputs using 2 Hidden Layers, (C) 2 Inputs, 9 Outputs using 1 Hidden Layer, (D) 2 Inputs, 9 Outputs using 2 Hidden Layers

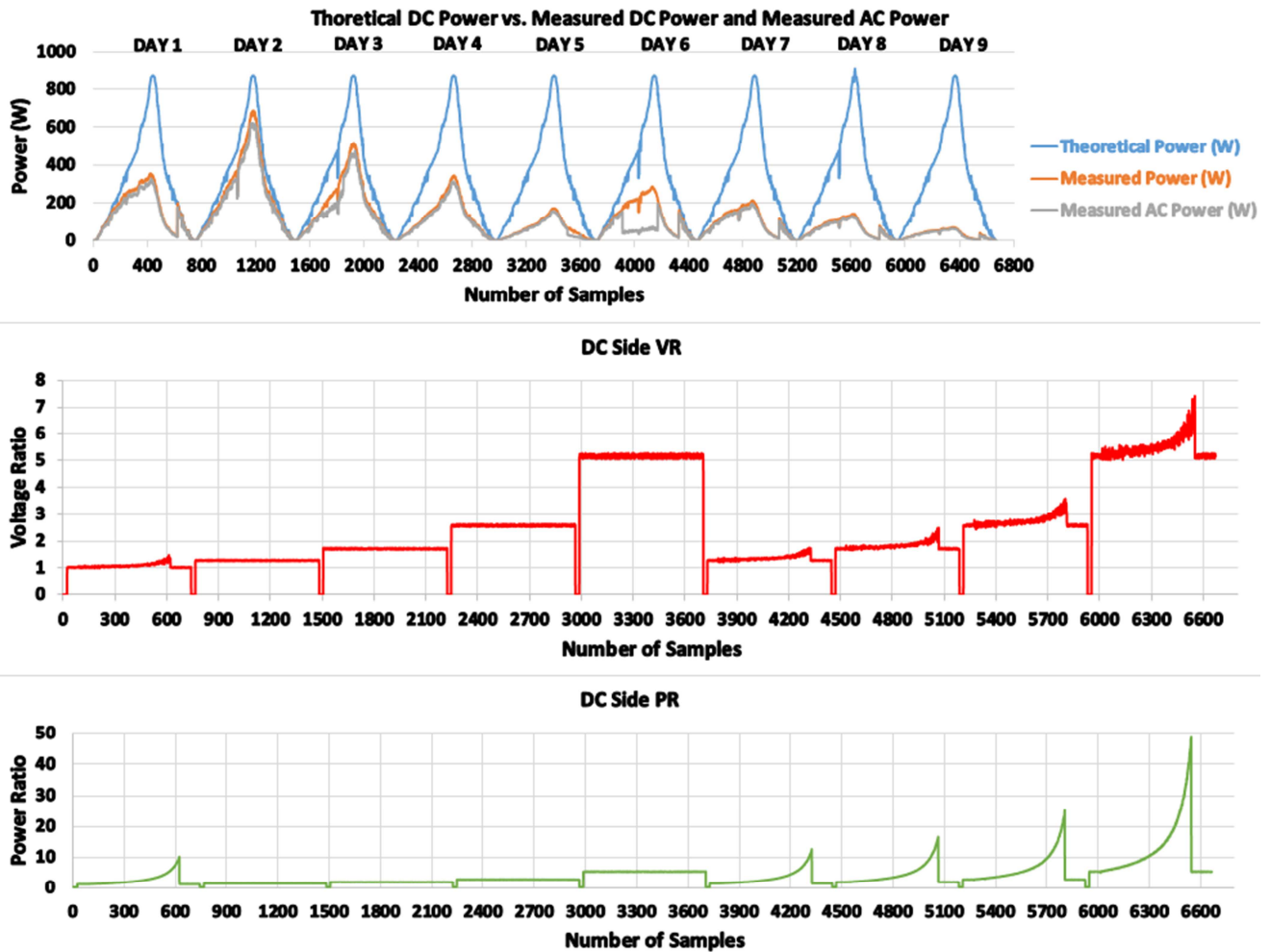


Fig. 7. Dataset used to Train and Validate the ANN networks

### 281 3.5 Fuzzy Logic Model Implementation

282 In this study, the second machine learning technique used to detect faults in the PV system is the fuzzy  
 283 logic system interface. In order to select the most efficient model for the fuzzy logic system fault  
 284 detection interface, a comparison between two fuzzy models widely utilized for the classification of faults  
 285 have been performed: Mamdani fuzzy logic and Sugeno type fuzzy system.

286 Mamdani fuzzy logic systems commonly suited to human input interface. However, the Sugeno fuzzy  
 287 systems are well established using a linear weighted mathematical expressions. The main advantages for  
 288 both fuzzy logic systems are illustrated by the following:

#### 289 Sugeno-type:

- 290 - It is computational efficient.
- 291 - It works well with linear techniques.
- 292 - It works well with optimization methods and
- 293 Adaptive techniques.
- 294 - It has guaranteed continuity of the output
- 295 Interface surface.

#### Mamdani-type:

- It is intuitive.
- It has widespread acceptance.
- It is well suited to human input
- systems interface

Both implemented fuzzy logic systems are shown in Fig. 8. The VR and PR ratios are used as input variables for the fuzzy logic classification system, where VR and PR is calculated using (7 & 9) respectively. The VR and PR regions are illustrated in Table 3. As can be noticed, ten different regions have been selected, where region 1 is the low partial shading (PS) condition. Whereas, region 4 is used for a faulty PV module with high PS condition (50% ~ 97.3% PS). The minimum and maximum limits for each region of the VR and PR is also shown in Table 3, the defuzzification process for the input rules is the centroid type.

All measurements for the theoretical VR and PR have been taken from a MATLAB/Simulink model which is designed the same as the examined PV system presented in Fig. 2 with the consideration of all PV parameters given in Table 2.

After identifying the input variables VR and PR regions, it is required to set the rulers for the fuzzy logic system interface. As shown in Fig 8, Mamdani fuzzy logic system consists of ten different membership functions (MF) which are described by the following:

- MF1: Low PS affecting the PV system
- MF2: High PS affecting the PV system
- MF3: One faulty PV module and low PS affecting the PV system
- MF4: One faulty PV module and high PS affecting the PV system
- MF5: Two faulty PV modules and low PS affecting the PV system
- MF6: Two faulty PV modules and high PS affecting the PV system
- MF7: Three faulty PV modules and low PS affecting the PV system
- MF8: Three faulty PV modules and high PS affecting the PV system
- MF9: Four faulty PV modules and low PS affecting the PV system
- MF10: Four faulty PV modules and high PS affecting the PV system

The Mamdani based system architecture is using the Max-Min composition technique with a centroid type defuzzification process.

TABLE 3  
FUZZY LOGIC INPUT REGIONS – VR & PR

Scenario	Partial Shading %	Min Voltage (V)	Max Voltage (V)	Min Power (W)	Max Power (W)	Fuzzy Classification System Region
Partial Shading (PS)	0 - 49%	1	1.2	1	2.4	1
	50 - 97.3%	1.1	1.4	2.1	28	2
Faulty PV Module and PS	0 - 49%	1.26	1.5	1.3	3	3
	50 - 97.3%	1.34	1.7	2.7	35	4
2 Faulty PV Module and PS	0 - 49%	1.67	1.95	1.8	4	5
	50 - 97.3%	1.76	2.26	3.5	47	6
3 Faulty PV Module and PS	0 - 49%	2.52	2.93	2.5	5.9	7
	50 - 97.3%	2.65	3.4	5.3	70	8
4 Faulty PV Module and PS	0 - 49%	5	5.9	5	12	9
	50 - 97.3%	5.3	6.8	10.6	141	10

321 Similarly, the fuzzy logic rules obtained for the Sugeno type fuzzy logic interface is equal to 10 as shown  
 322 in Fig. 8. Where each rule presents the same rule as described in the Mamdani fuzzy logic system. The  
 323 Sugeno based system architecture is using the Max-Min composition technique with a centroid type  
 324 defuzzification process.

325 It is worth pointing out that a high number of fuzzy logic rules ensure both completeness and appropriate  
 326 resolution of the fault detection accuracy. However, a high number of fuzzy rules may lead to an over  
 327 parameterized system, thus reducing generalization capability and accuracy of detection the type of the  
 328 fault accruing in the examined PV system. Therefore, the number of fuzzy rules depends on the number  
 329 of input variables, system performance, the execution time and the membership functions. In this paper,  
 330 ten fuzzy logic rules were decided according to a sensitivity analysis made by varying the number and  
 331 type of the rule. A satisfactory level of performance was obtained after a tuning process, i.e. starting from  
 332 faulty PV module only and progressively modifying the fuzzy system to detect all possible faults the may  
 333 occur in the PV plant according to the faults types listed in Table 1.

334 Both fuzzy logic systems rules are based on: if, and statement. The fuzzy rules are briefly listed in  
 335 Appendix A. Furthermore, the output surface for Mamdani and Sugeno fuzzy logic systems are plotted  
 336 and represented by a 3D curves as shown in Fig. 9(A) and Fig. 9(B) respectively. Where the x-axis  
 337 presents the PR ratio, y-axis presents the VR ratio, and the fault detection output is on the z-axis.

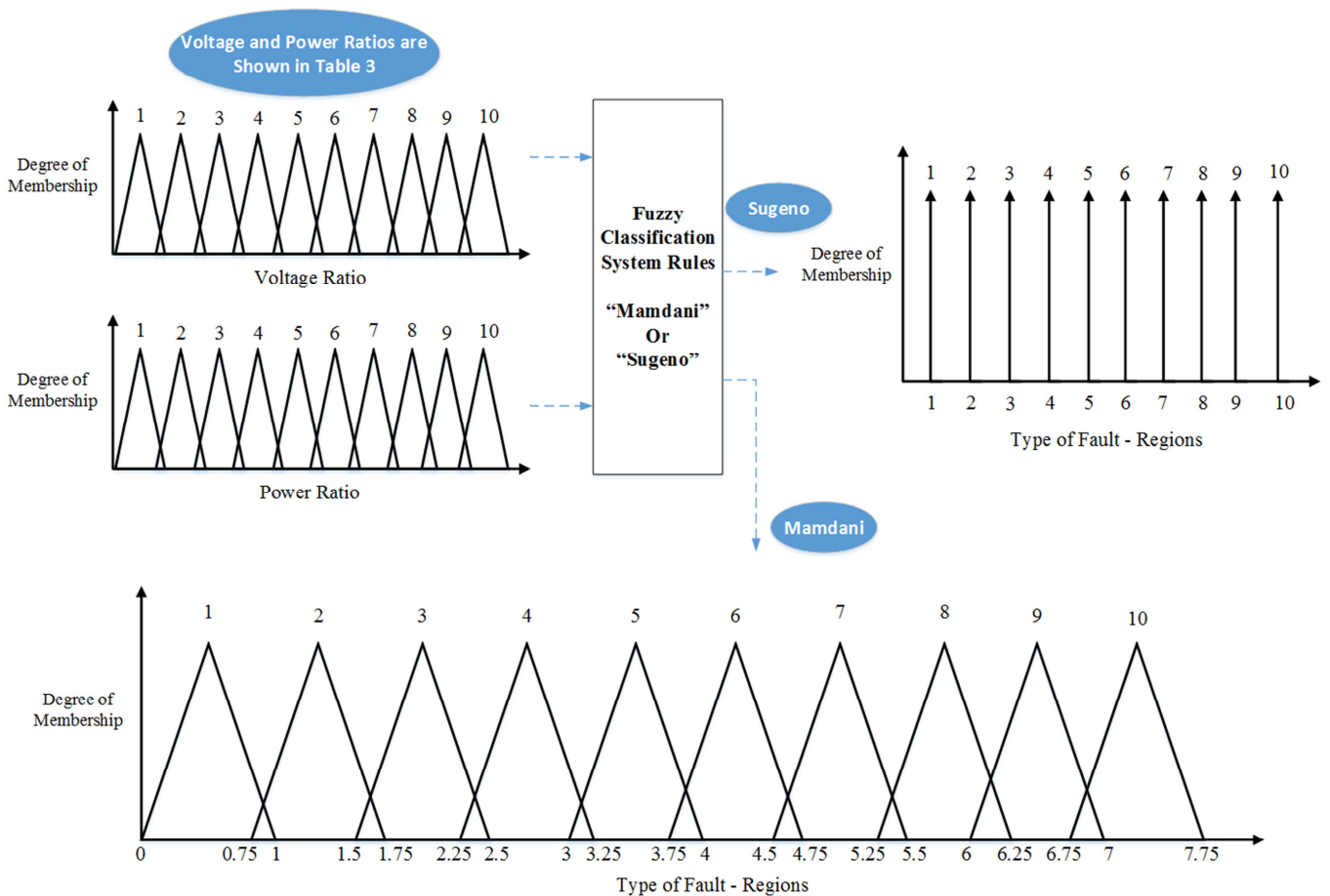


Fig. 8. The Adopted Sugeno and Mamdani Fuzzy Logic Systems

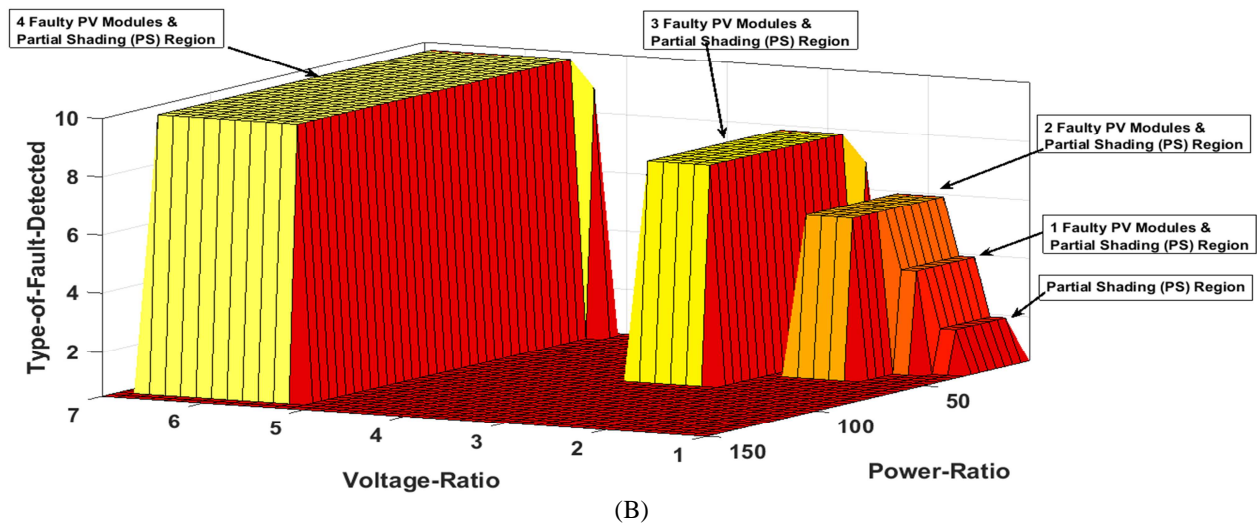
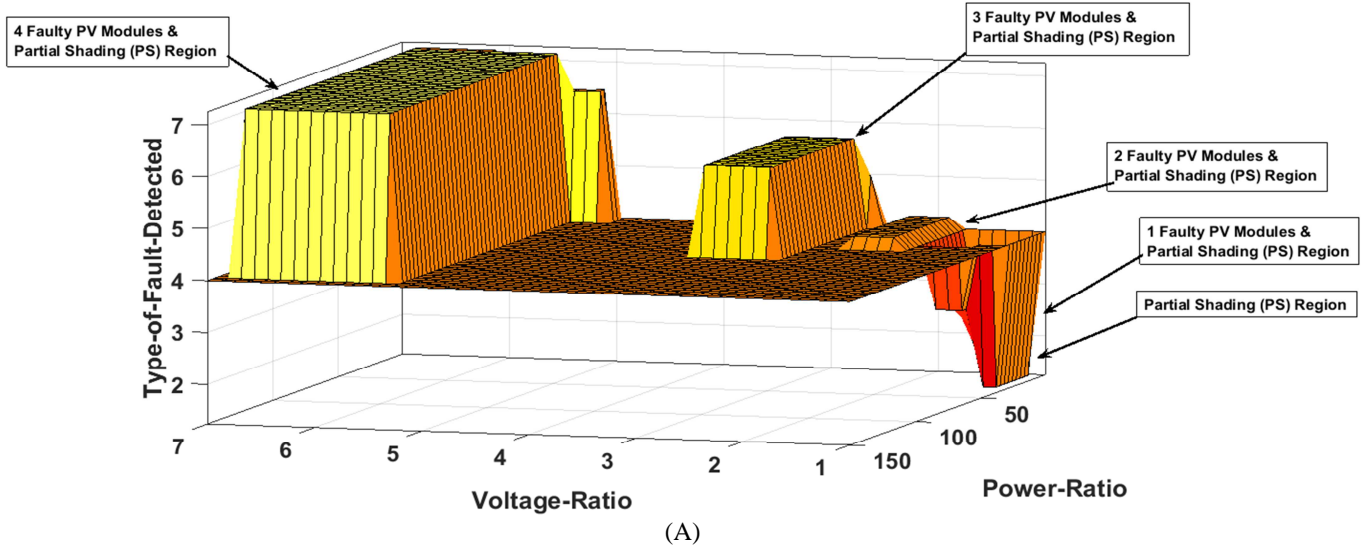


Fig. 9. Fuzzy Logic Systems Classifier Output Surfaces. (A) Mamdani-Type Fuzzy Logic System Interface, (B) Sugeno-Type Fuzzy Logic System Interface

#### 338 4. RESULTS AND DISCUSSION

339 This section reports the results of the developed fault detection algorithm. Furthermore, a comparison  
 340 between the developed machine learning techniques with some ANN and fuzzy logic systems obtained by  
 341 various researchers is briefly explained in section 4.4 (discussion section).

##### 342 4.1 Experimental Data

343 In order to test the effectiveness of the proposed fault detection algorithm, a number experiments were  
 344 conducted. Table 4 shows a full day experimental scenarios which are applied to the PV plant, where the  
 345 perturbation process made to the PV system is shown in Appendix B. Each scenario lasts for an hour and  
 346 it contains a different condition applied to the examined PV system illustrated previously in Fig. 2.

347 As can be noticed, the data samples for both sleep and normal operation modes are not included in the  
 348 evaluation process of the machine learning techniques, since both scenarios can be detected using the  
 349 mathematical regions explained in Fig. 5. Furthermore, scenarios 3~5 and 7~11 are evaluated by the ANN  
 350 network and the fuzzy logic system, where the total number of sample for the faulty conditions is equal to

351 four hundred and eighty. Moreover, a comparison between the theoretical output power vs. the real time  
 352 long term measured data of the PV system during the tested faulty conditions are is shown in Fig. 10.

TABLE 4  
 MULTIPLE FAULTS OCCURRING IN THE EXAMINED PV SYSTEM

Scenario #	Start time	End time	Condition applied to the PV system	Number of samples applied to the ANN network
1	5:45	5:57	Sleep mode	-
2	5:58	6:59	Normal operation mode	-
3	7:00	7:59	20% partial shading	60
4	8:00	8:59	Faulty PV module and 20% partial shading	60
5	9:00	9:59	Faulty PV module and 40% partial shading	60
6	10:00	10:59	Normal operation mode	-
7	11:00	11:59	2 Faulty PV modules and 30% partial shading	60
8	12:00	12:59	30% partial shading	60
9	13:00	13:59	4 Faulty PV modules only	60
10	14:00	14:59	3 Faulty PV modules and 20% partial shading	60
11	15:00	15:59	3 Faulty PV modules only	60
12	16:00	17:57	Normal operation mode	-
13	17:58	19:00	Sleep mode	-
				Sum: 480

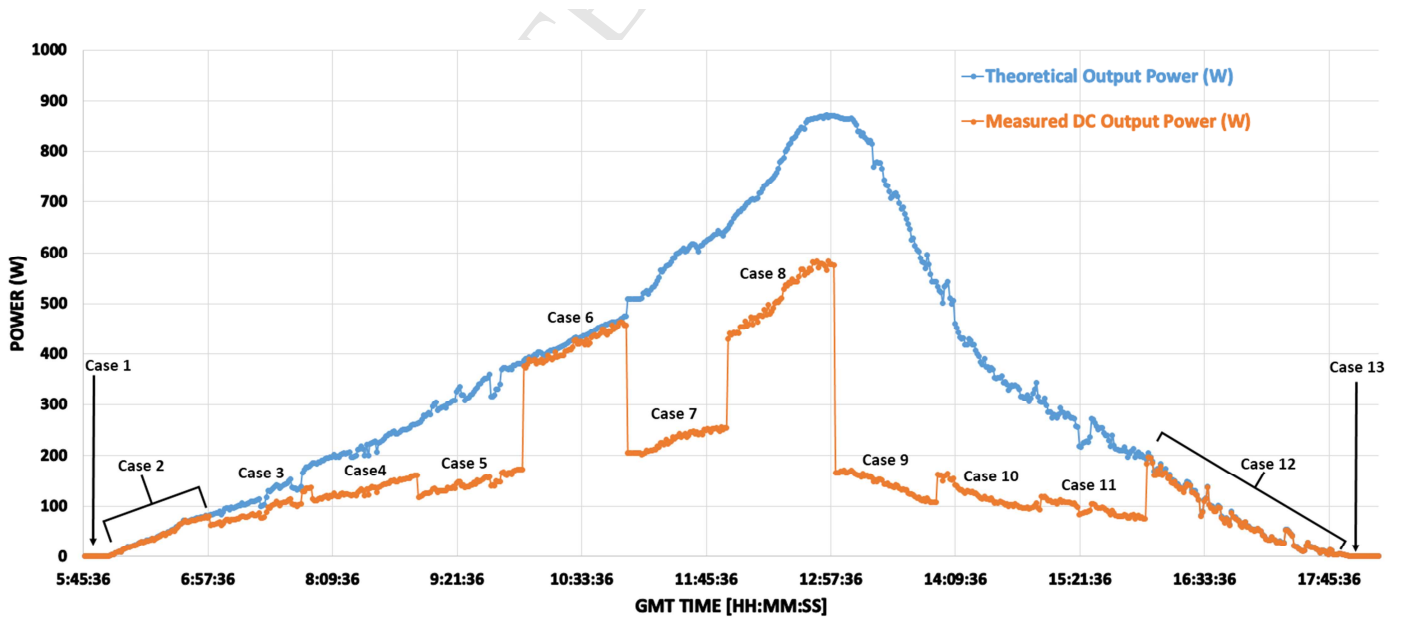


Fig. 10. Theoretical Output Power vs. Measured Output Power for All Tested Scenarios Applied on the Examined PV system, Each Case is Perturbed as Shown in Appendix B

## 353 4.2 Performance Evaluation of the proposed ANN Networks

354 In order to verify the performance of the proposed ANN networks, the VR and PR ratios of 480 samples  
 355 illustrated in Table 4 have been used as an input for each ANN network shown previously in Fig. 6. For  
 356 analyzing the effectiveness of each ANN network, Fig 11(A-D) shows the output classification confusion  
 357 matrices for the developed ANN networks.

358 The cells of each matrix with red and green colors presents the percentage of faults correctly and not  
 359 correctly classified by the ANN network respectively. Additionally, the fault classification number, fault  
 360 type and number of samples for each examined ANN network is shown in Table 5. Moreover, the gray  
 361 blocks represents the total percentage of the detection accuracy in the column and row respectively.

362 In order to understand how to read the confusion matrices shown in Fig. 11. The first confusion matrix  
 363 (Fig. 11(A)) will be explained in brief. In this figure, the first five diagonal cells show the number and  
 364 percentage of correct classifications by the trained network. For example, 118 samples for F1 (fault type,  
 365 shown in Table 5), are correctly classified. This corresponds to 24.6% of all tested samples (480 sample).  
 366 Similarly, 30 samples are correctly classified as F2, this corresponds to 6.3% of all 480 samples.

367 In row 1, 1 sample is incorrectly classified as F1 and it is classified as F3, this corresponds to 0.2% of all  
 368 480 samples. Similarly, 2 samples of F5 are incorrectly classified as F1 and this corresponds to 0.4% of  
 369 all 480 samples.

370 In row 2, 30 samples are correctly classified as being F2, this corresponds to 6.3% of all 480 samples.

371 Out of 120 sample corresponds to row 1, 97.5% are correct and 2.5% are wrong. Out of 120 samples  
 372 corresponds to column 1, 98.3% are correct and 1.7% are classified incorrectly. For row 2, all samples  
 373 have been classified correctly, 100%. However, for column 2, out of 120 samples, 25% are correct and  
 374 75% are incorrect.

375 The overall detection accuracy of the confusion matrix could be calculated using the diagonal cells as the  
 376 following:

377

$$378 \quad 1^{\text{st}} \text{ cell (24.6\%)} + 2^{\text{nd}} \text{ cell (6.3\%)} + 3^{\text{rd}} \text{ cell (10.2\%)} + 4^{\text{th}} \text{ cell (17.3\%)} + 5^{\text{th}} \text{ cell (11.9\%)} = 70.2\%$$

379

380 This 70.2 corresponds to the percentage of correctly classified samples (out of all tested samples, 480  
 381 sample). And 29.8% correspond to incorrectly classified samples.

382 From the obtained results in Fig. 11(A) the minimum detection accuracy is associated with column 2,  
 383 where 75% of the samples are incorrectly classified. This situation occurred when 3 faulty PV modules  
 384 and PS affecting the PV module (F3) is classified as F2. And this happens when there is a rapid  
 385 drop/increase in the irradiance level or PS conditions affecting the examined PV modules.

386 Similar results obtained with the second ANN network (contains 2 outputs and 2 hidden layers) shown in  
 387 Fig. 11(B). Where the percentage of the error in identifying F3 is increased to 83.3%, shown in column 2.  
 388 However, the overall detection accuracy of the second ANN network is increased to 77.7% comparing to  
 389 70.2% obtained by the first ANN network. This increase in the detection accuracy is due to the second  
 390 hidden layer which enables more training and validation computational process for the ANN network  
 391 before the testing phase.

392 As can be noticed, ANN networks one and two have low overall detection accuracy. As mentioned earlier  
 393 in section 3.4, this challenge was solved by adding new type of faults for the ANN network that allows  
 394 the ANN model to detect faulty PV modules only (No PS on the entire PV plant).

395 Fig. 11(C) describes the output classification confusion matrix of the third ANN network (contains 9  
 396 outputs and 1 hidden layer). The overall detection accuracy of the ANN network is equal to 87.5% where  
 397 the highest error is associated with F7 (row 7). This fault is related to the samples of F7 which are  
 398 classified as F8. This situation occurred when two faulty PV modules with high partial shading condition  
 399 is detected by the ANN network as three faulty PV modules with low PS condition affecting the entire PV  
 400 system.

401 The last ANN network contains 2 inputs, 9 outputs and 2 hidden layers. The overall detection accuracy of  
 402 the network is 92.1% which means that the ANN network detects accurately 442 samples out of 480, this  
 403 results is shown in Fig. 11(D).

404 The highest error in identifying the type of the fault is associated with the samples of F6 being classified  
 405 as F1. The total percentage of error is equal to 10.3%, shown in column 1. Out of 120 samples, 8 sample  
 406 are incorrectly classified. This situation occurred when there is a high partial shading conditions applied  
 407 to the PV system including one faulty PV module. Based on the detected samples, this type of the fault is  
 408 classified as being F1 (PS affecting the PV system).

409 In conclusion, the obtained results of this section shows that the maximum detection accuracy of all  
 410 examined ANN networks is equal to 92.1% which is achieved by the fourth ANN network that includes 2  
 411 inputs, 9 outputs with 2 hidden layers.

TABLE 5  
 FAULTS ASSOCIATED WITH THE EXAMINED ANN NETWORKS

ANN network	Fault number	Type of the fault	Number of samples
ANN network 1 and 2 as shown in Fig. 11(A) and Fig. 11(B) respectively	F1	PS affecting the PV system	120
	F2	1 Faulty PV module & PS affecting the PV module	120
	F3	2 Faulty PV modules & PS affecting the PV module	60
	F4	3 Faulty PV modules & PS affecting the PV module	120
	F5	4 Faulty PV modules & PS affecting the PV module	60
ANN network 3 and 4 as shown in Fig. 11(C) and Fig. 11(D) respectively	F1	PS affecting the PV system	120
	F2	1 Faulty PV module	0
	F3	2 Faulty PV modules	0
	F4	3 Faulty PV modules	60
	F5	4 Faulty PV modules	60
	F6	1 Faulty PV module & PS affecting the PV module	120
	F7	2 Faulty PV modules & PS affecting the PV module	60
	F8	3 Faulty PV modules & PS affecting the PV module	60
	F9	4 Faulty PV modules & PS affecting the PV module	0

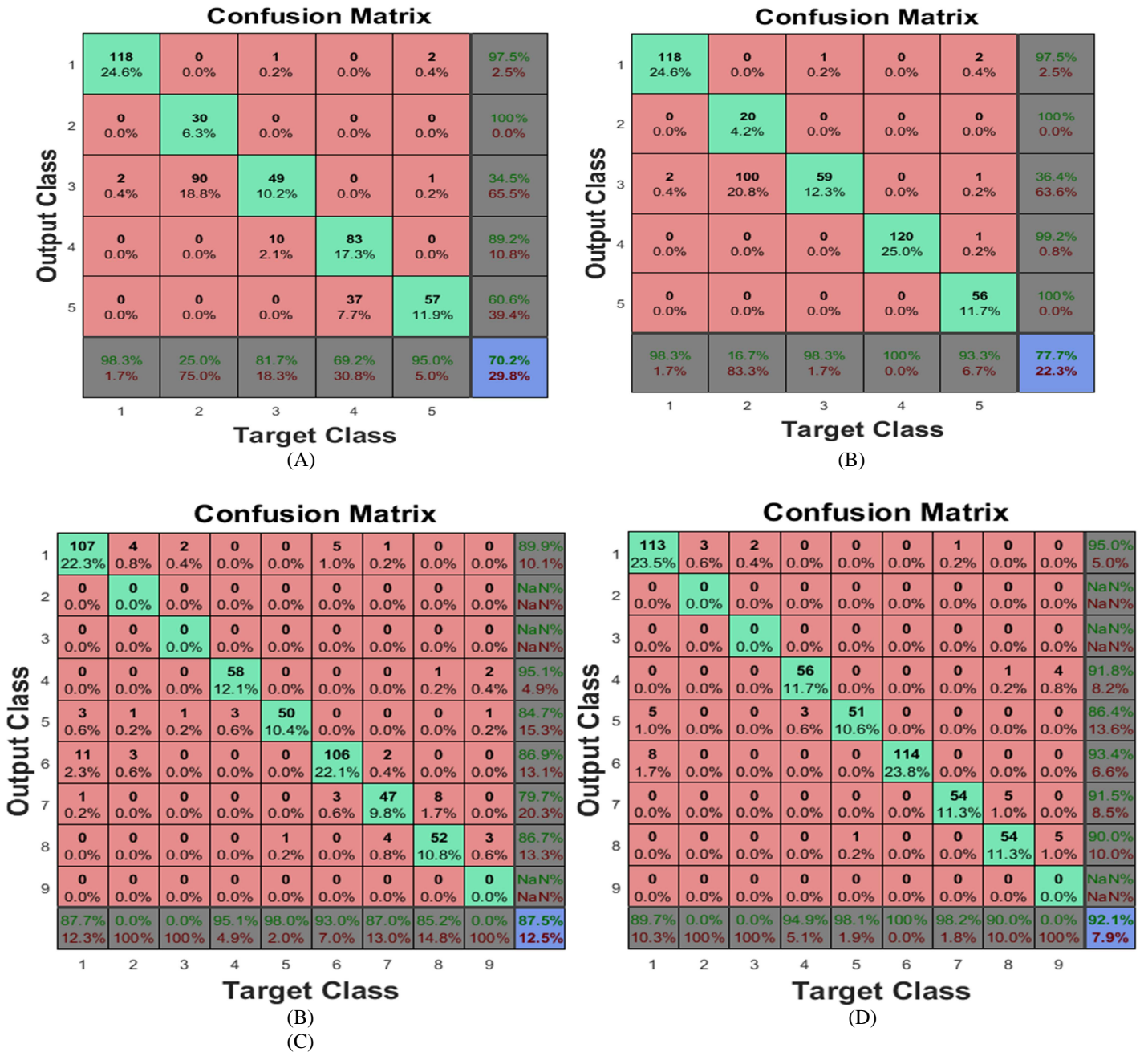


Fig. 11. Classification Confusion Matrices for the Examined ANN Networks shown previously in Fig. 4. (A) 2 Inputs, 5 Outputs using 1 Hidden Layer, (B) 2 Inputs, 5 Outputs using 2 Hidden Layers, (C) 2 Inputs, 9 Outputs using 1 Hidden Layer, (D) 2 Inputs, 9 Outputs using 2 Hidden Layers

### 412 4.3 Performance Evaluation of the proposed Fuzzy Logic Systems

413 In order to test the effectiveness of the proposed fuzzy logic systems (Mamdani and Sugeno) the faulty  
 414 samples shown previously in Table 4 have been processed in each fuzzy system. Furthermore, the  
 415 implementation of the fuzzy logic systems are explained in section 3.5.

#### 416 A. Mamdani Fuzzy Logic System:

417 Fig. 12(A) shows the output membership function vs. the faulty samples which are equal to 480 for  
 418 Mamdani fuzzy logic system interface. Each faulty PV condition is labelled on the figure. As an example,

419 case 3 presents 20% partial shading condition affecting the PV module, for this particular PV faulty  
 420 scenario, the output of the fuzzy system is equal to 0.5, which is the region of PS condition illustrated in  
 421 Fig. 12(B). Similarly, case 4 and 5 presents a faulty PV module with 20% and 40% PS respectively. Both  
 422 cases are within the same membership function region due to the low PS condition affecting the PV  
 423 modules, this situation is labeled as case 4 and case 5 on both Figs. 12(A) and 12(B).

424 As can be noticed that all examined faulty conditions are accurately detected by Mamdani fuzzy logic  
 425 system. However, between case 7 and case 8 there is a small amount of error in detecting the region of the  
 426 fault, same result accruing between case 8 and case 9. This situation is occurring in the fuzzy system due  
 427 to the high number of faulty regions identified by the fuzzy system, additionally, the VR and PR ratios are  
 428 strongly depends on the performance of the voltage and current sensors used to detect the change in the  
 429 PV parameters (voltage, current and power). Therefore, the fuzzy logic system might need some extra few  
 430 seconds to start detecting the exact faulty occurring in the PV installation.

### 431 B. Sugeno Fuzzy Logic System:

432 Fig. 13(A) shows the output membership function vs. the faulty samples for Sugeno fuzzy logic system  
 433 interface. Each faulty PV condition is labelled on the figure. As an example, case 7 presents two faulty  
 434 PV modules and low partial shading condition affecting the PV plant, for this particular PV faulty  
 435 scenario, the output of the fuzzy system is equal to 5, which is the region of PS condition illustrated in

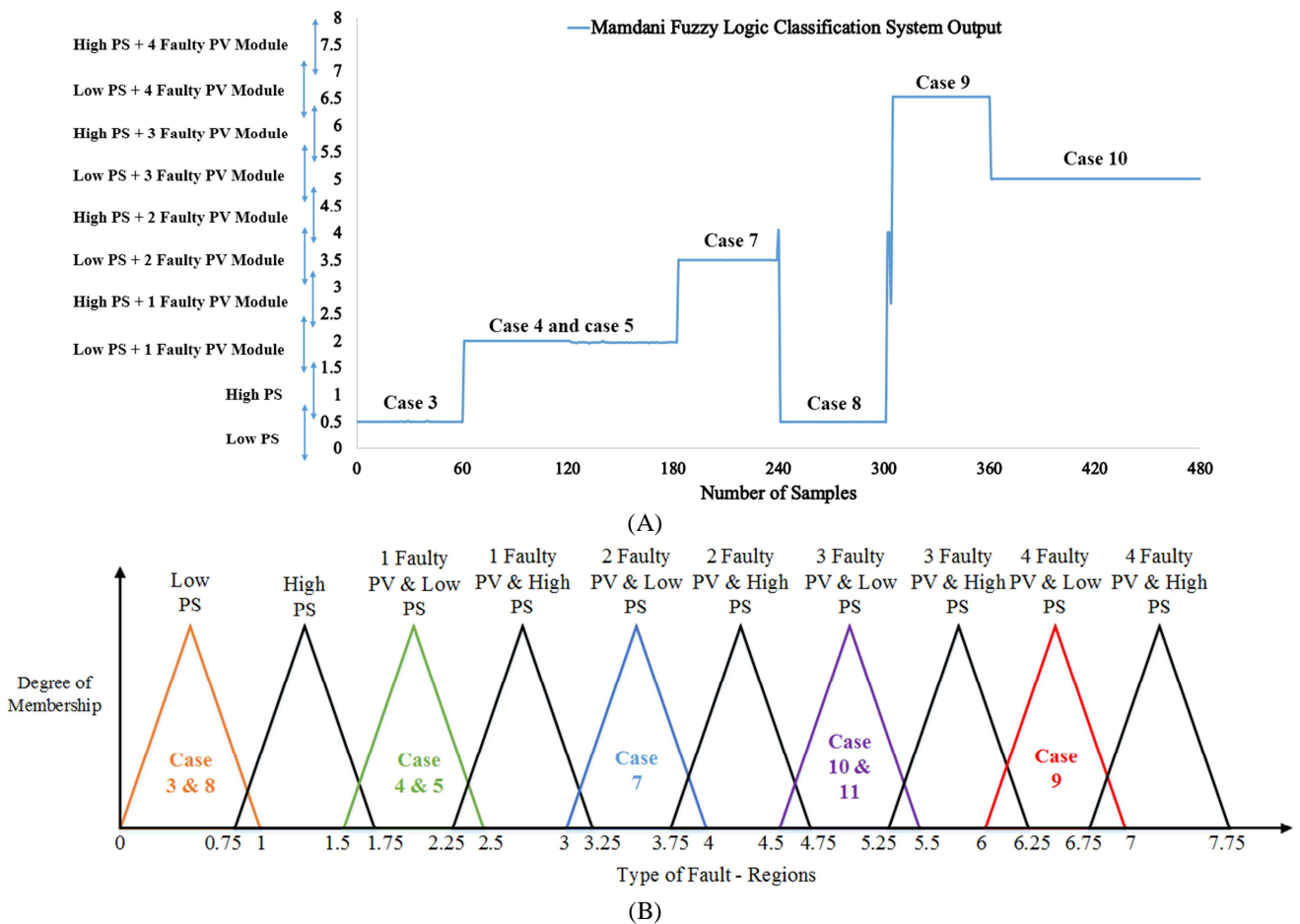


Fig. 12. Output Results Obtained using Mamdani Fuzzy Logic System. (A) Membership Functions vs. Number of Samples, (B) Membership Function Explained Previously in Section 3.5 vs. Type of Fault

436 Fig. 13(B). Similarly, case 10 and 11 presents a three faulty PV modules with 20% and 0% PS  
 437 respectively. Both cases are within the same membership function region due to the low PS condition  
 438 affecting the PV modules, this situation is labeled as case 10 and case 11 on both Figs. 13(A) and 13(B).

439 From the result obtained by the Sugeno fuzzy logic system, all examined faulty conditions are accurately  
 440 detected. However, between case 7 and case 8 there is a small amount of error in detecting the region of  
 441 the fault. This situation is occurring in the fuzzy system due to the high number of faulty regions  
 442 identified by the fuzzy system, additionally, the VR and PR ratios are strongly depends on the  
 443 performance of the voltage and current sensors used to detect the change in the PV parameters (voltage,  
 444 current, and power). Similar error was also observed by the Mamdani fuzzy logic system between case 7  
 445 and case 8.

446 In conclusion, this section presents the behavior of the fuzzy logic systems developed for detecting faulty  
 447 conditions occurring in the examined PV system. Both fuzzy logic systems show an accurate results in  
 448 detecting various faults comparing to the results obtained by the ANN networks which has a maximum  
 449 detection accuracy equals to 92.1%. A comparison between both machine learning techniques are

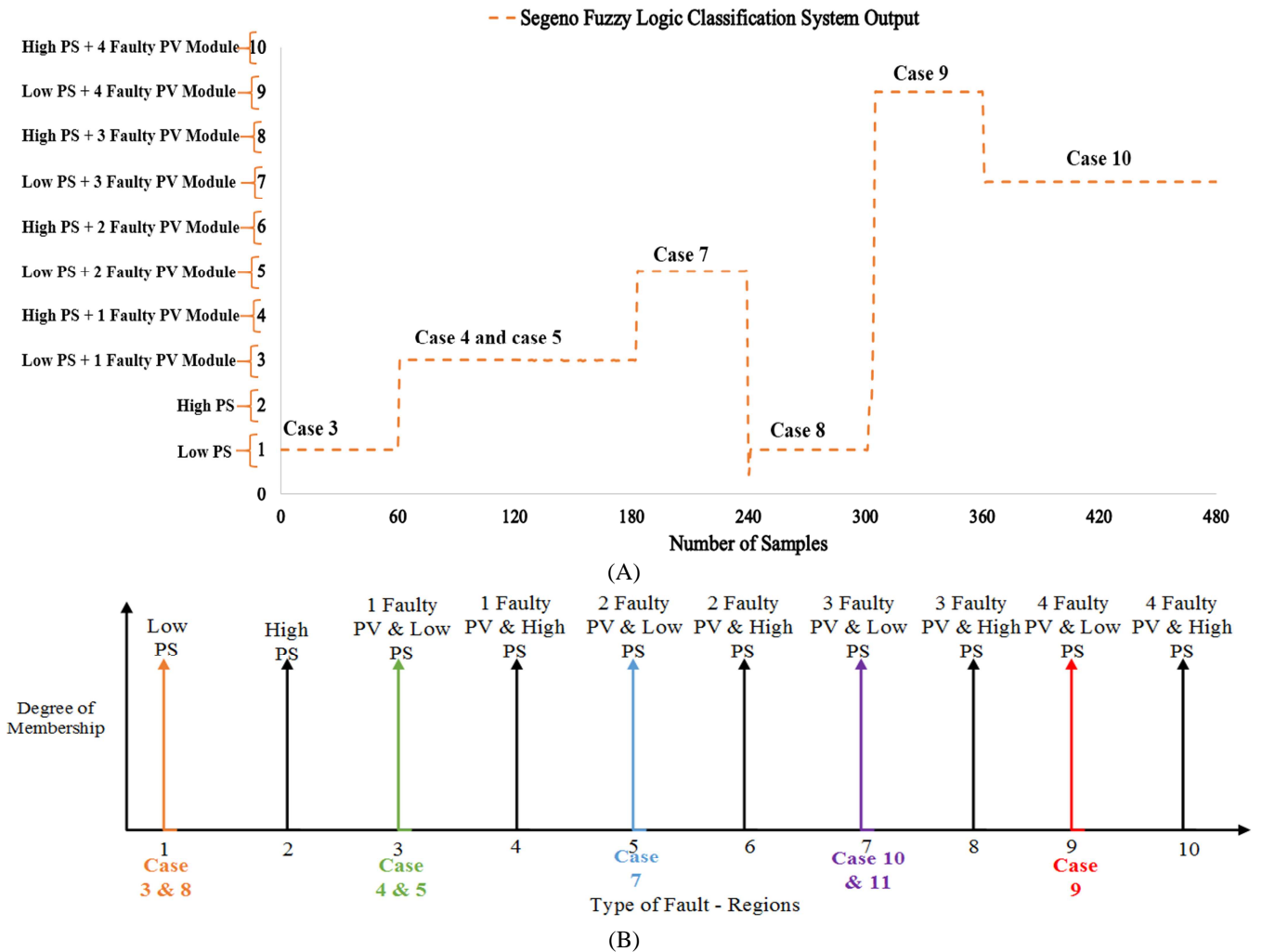


Fig. 13. Output Results Obtained using Sugeno Fuzzy Logic System. (A) Membership Functions vs. Number of Samples, (B) Membership Function Explained Previously in Section 3.5 vs. Type of Fault

450 discussed briefly in the following section: 4.4 discussion.

#### 451 4.4 Discussion

452 In this study, artificial intelligent network (ANN) and fuzzy logic system interface have been developed  
 453 for detecting faults in PV installations. However, the PV system used for analyzing the performance of  
 454 both machine learning techniques is considered as low capacity PV installation (1.1 kWp). For that  
 455 instance, the output of the fuzzy logic systems shows an accurate detecting accuracy (all examined faults  
 456 have been detected correctly) comparing to the ANN which has a maximum detection accuracy equals to  
 457 92.1% obtained for the fourth ANN structure which contains 2 inputs, 9 outputs using 2 hidden layers.  
 458 The input membership functions of the fuzzy logic system could be much complicated if the examined  
 459 PV installation has much more PV modules (~100 PV modules), since each PV module could affect the  
 460 overall input membership functions.

461 In order to test the effectiveness of the final detection accuracy obtained by the ANN network. The  
 462 proposed method has been compared with the ANN output results presented in [25]. The output confusion  
 463 matrix for both obtained studies are compared in Fig. 14(A) and Fig. 14(B). As can be noticed, the overall  
 464 detection efficiency of the proposed ANN network is equal to 92.1% comparing to 90.3% obtained by  
 465 [25]. The faults which are detected by [25] is related to the bypass diodes in the PV systems which is  
 466 quite different than the faults obtained by this research. However, both ANN networks are using the  
 467 variations of the voltage and the power form the PV plant as an inputs for the ANN model.

468 To the best of our knowledge, few of the reviewed articles used a fuzzy logic system to detect faults in  
 469 PV installations. Therefore, this is one of the novel contribution of this study. A comparison between the  
 470 output membership functions developed by [1] and this study are shown in Fig. 15(A) and Fig. 15(B)  
 471 respectively. In [1] authors' are using Mamdani fuzzy logic system for enhancing the detection of partial  
 472 shading conditions effecting the PV plant. The proposed mathematical calculations of the fuzzy logic  
 473 system is also presented in Fig. 15(A). Moreover, the fuzzy logic systems (Mamdani and Sugeno)  
 474 presented in this paper are used for detecting possible faults accruing in the examined PV system. The  
 475 overall detection accuracy of the proposed fuzzy systems is very high, since the examined PV system

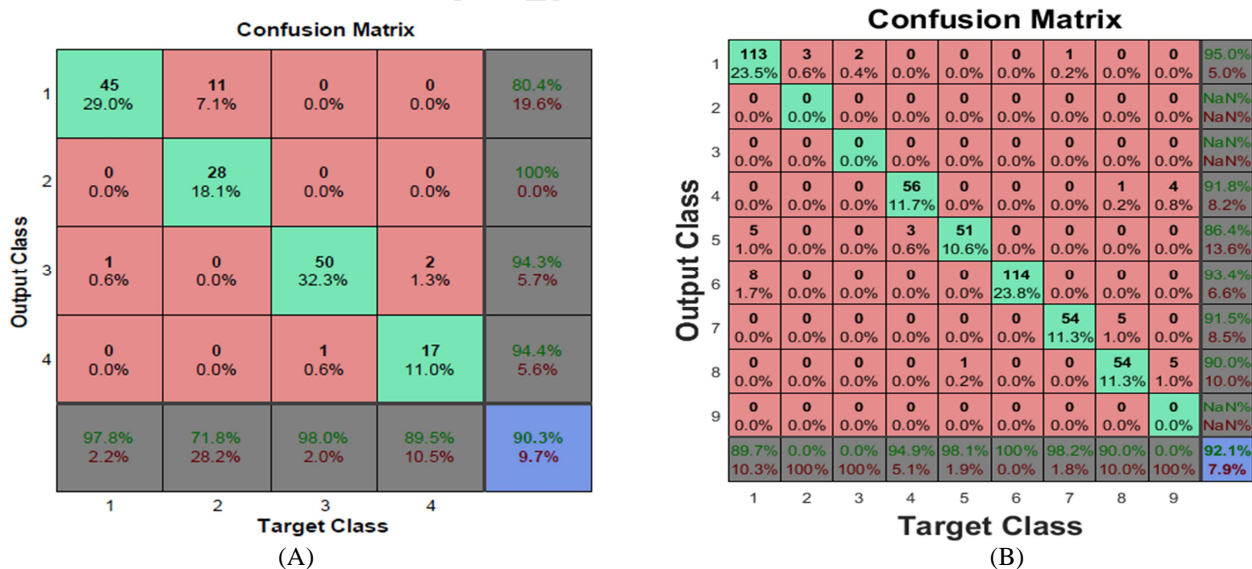
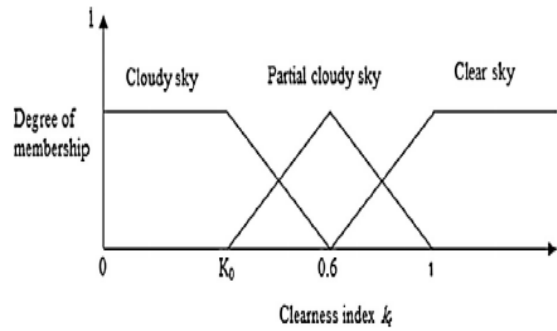


Fig. 14. Classification Confusion Matrix for ANN Network. (A) Results Obtained by W. Chine et al [25], (B) Results Achieved using the Proposed ANN Fault Detection Algorithm

Clear sky :  $R_{ib} \leq R_c : k_t = 1$

Partially covered sky :  $R_c < R_{ib} < R_n : k_t = 1 - (1 - K_0) \frac{(R_{ib} - R_c)}{(R_n - R_c)}$

Completely covered sky :  $R_{ib} \geq R_n : k_t = K_0$



1. Low PS
2. High PS
3. 1 Faulty PV & Low PS
4. 1 Faulty PV & High PS
5. 2 Faulty PV & Low PS
6. 2 Faulty PV & High PS
7. 3 Faulty PV & Low PS
8. 3 Faulty PV & High PS
9. 4 Faulty PV & Low PS
10. 4 Faulty PV & High PS

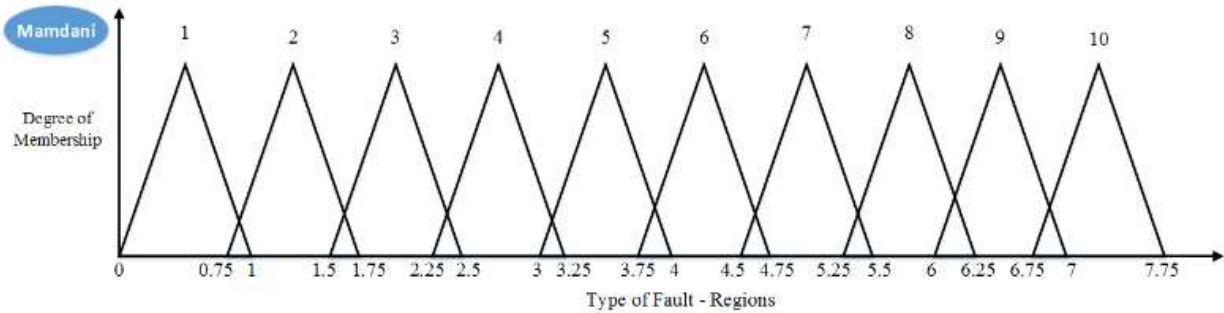
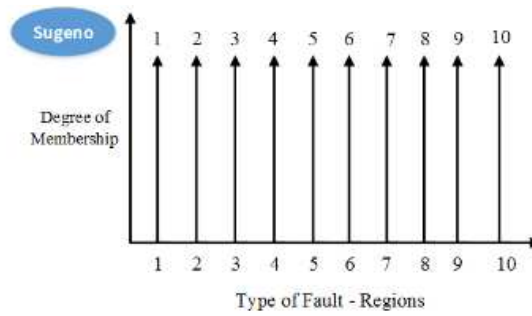


Fig. 15. Fuzzy Logic Models. (A) Membership Functions Proposed by M. Tadj [1], (B) Membership Functions for Mamdani and Sugeno Fuzzy Logic Systems Proposed in this Study

476 does not contain too many PV modules.

477 The obtained results for the developed ANN network and the fuzzy logic system are compared in Table 5.  
 478 The mathematical modelling on the ANN network is much simpler comparing to the creation of the fuzzy  
 479 logic membership functions, this situation is correct specially for large PV installations. However, the  
 480 ANN network does require a log of samples in order to validate and train the network while the fuzzy  
 481 logic systems does not require any log of data before creating the membership function, it just need to  
 482 update the mathematical modelling with the degradation rates of the MPPT units and/or any other  
 483 possible source for decreasing the overall efficiency of the PV system such as the DC/AC inverters.

TABLE 6  
COMPARISON BETWEEN ANN AND FUZZY LOGIC SYSTEMS

Comparison	ANN Network Fault Detection Approach	Fuzzy Logic System Fault Detection Approach
Mathematical Modelling	Does not contain complex mathematical modelling, since it depends on a log of data	For larger PV systems(~100 PV modules) the membership functions does require a lot of mathematical expressions
Detection Accuracy	High	High
Detection Time “Response”	Fast (milli/micro seconds)	Fast (milli/micro seconds)
Photovoltaic Parameters	Depends on the type of the PV fault which needs to be detected	Depends on the type of the PV fault which needs to be detected
Logged Data	Required	Dose not require any previous logged data
Recent Applications Applied to PV Systems	<ul style="list-style-type: none"> <li>i. Improving the estimation of GCPV power output [33]</li> <li>ii. Forecasting for global solar radiation [34 &amp; 35]</li> </ul>	<ul style="list-style-type: none"> <li>i. Power optimization in standalone PV systems [21]</li> <li>ii. PV fault detection based on multi-resolution signal decomposition [36 &amp; 37]</li> </ul>

484 The overall detection accuracy for both machine learning techniques are high if they have been built  
 485 accurately. Finally, Table 6 shows some of the recent applications for ANN networks and the fuzzy logic  
 486 systems developed nowadays in PV plants.

## 487 5. CONCLUSION

488 This paper presents a new photovoltaic (PV) fault detection algorithm which comprises both artificial  
 489 neural network (ANN) and fuzzy logic system interface. The algorithm is capable for detecting various  
 490 fault occurring in the PV system such as faulty PV module, two faulty PV modules and partial shading  
 491 conditions affecting the PV system. Both machine learning techniques was validated using a 1.1 kWp PV  
 492 plant installed at the University of Huddersfield, United Kingdom.

493 The fault detection algorithm is using the variations of the voltage and power of the examined PV system  
 494 as an input for both ANN and the fuzzy logic system. In order to achieve high rate of detection accuracy,  
 495 four various ANN networks have been tested. The maximum overall detection accuracy was obtained is  
 496 equal to 92.1% from an ANN network which contains 2 inputs, 9 outputs using 2 hidden layers.

497 Additionally, two different fuzzy logic systems have been examined. Mamdani fuzzy logic system  
 498 interface and Sugeno type fuzzy system. Both examined fuzzy logic systems show approximately the  
 499 same output during the experiments. However, there are slightly difference in developing each type of the  
 500 fuzzy systems such as the output membership functions and the rules applied for detecting the type of the  
 501 fault occurring in the PV plant

502 The developed fault detection algorithm has been discussed and compared with various results obtained  
503 from different references in the discussion section. Finally, further investigation of the proposed fault  
504 detection algorithm is intended to be used with field programmable gate array (FPGA) platforms which  
505 accelerate the speed of detecting possible faults occurring in PV systems.

#### 506 *Appendix A*

507 Fuzzy logic rules applied for both Mamdani and Sugeno fuzzy logic systems interface:

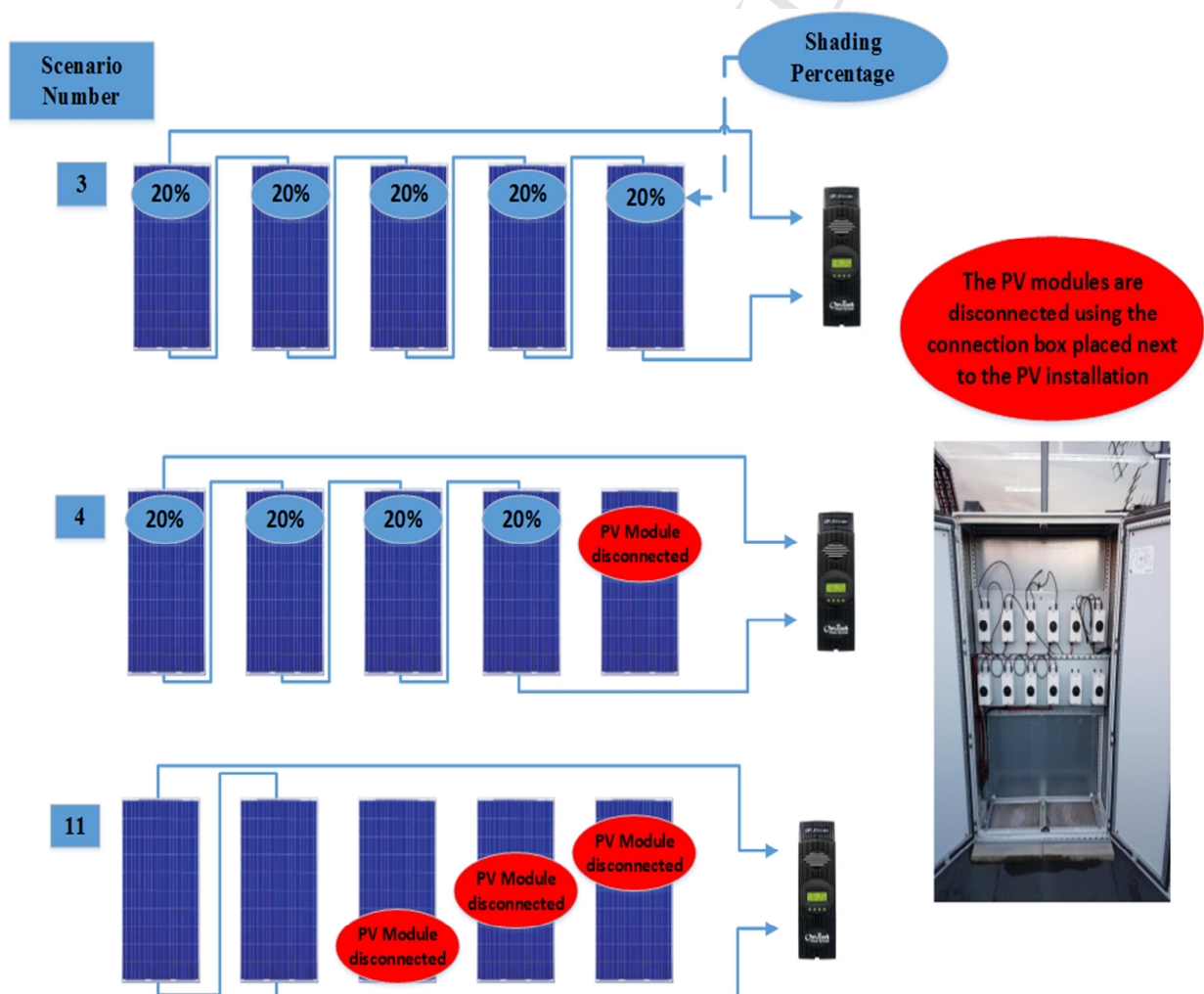
- 508 • 1. If (Voltage-Ratio is 1) and (Power-Ratio is 1) then (Type-of-Fault-Detected is 1) (1)
- 509 • 2. If (Voltage-Ratio is 2) and (Power-Ratio is 2) then (Type-of-Fault-Detected is 2) (1)
- 510 • 3. If (Voltage-Ratio is 3) and (Power-Ratio is 3) then (Type-of-Fault-Detected is 3) (1)
- 511 • 4. If (Voltage-Ratio is 4) and (Power-Ratio is 4) then (Type-of-Fault-Detected is 4) (1)
- 512 • 5. If (Voltage-Ratio is 5) and (Power-Ratio is 5) then (Type-of-Fault-Detected is 5) (1)
- 513 • 6. If (Voltage-Ratio is 6) and (Power-Ratio is 6) then (Type-of-Fault-Detected is 6) (1)
- 514 • 7. If (Voltage-Ratio is 7) and (Power-Ratio is 7) then (Type-of-Fault-Detected is 7) (1)
- 515 • 8. If (Voltage-Ratio is 8) and (Power-Ratio is 8) then (Type-of-Fault-Detected is 8) (1)
- 516 • 9. If (Voltage-Ratio is 9) and (Power-Ratio is 9) then (Type-of-Fault-Detected is 9) (1)
- 517 • 10. If (Voltage-Ratio is 10) and (Power-Ratio is 10) then (Type-of-Fault-Detected is 10) (1)

#### 518 *Appendix B*

519 Perturbation process made to test the examined photovoltaic plant:

520 **REFERENCES**

- 521 [1] Tadj, M., Benmouiza, K., Cheknane, A., & Silvestre, S. (2014). Improving the performance of PV systems  
522 by faults detection using GISTEL approach. *Energy conversion and management*, 80, 298-304.
- 523 [2] Mellit, A., & Pavan, A. M. (2010). A 24-h forecast of solar irradiance using artificial neural network:  
524 Application for performance prediction of a grid-connected PV plant at Trieste, Italy. *Solar Energy*, 84(5),  
525 807-821.
- 526 [3] Takashima, T., Yamaguchi, J., Otani, K., Oozeki, T., Kato, K., & Ishida, M. (2009). Experimental studies  
527 of fault location in PV module strings. *Solar Energy Materials and Solar Cells*, 93(6), 1079-1082.
- 528 [4] Dhimish, M., & Holmes, V. (2016). Fault detection algorithm for grid-connected photovoltaic plants. *Solar  
529 Energy*, 137, 236-245.
- 530 [5] Silvestre, S., Chouder, A., & Karatepe, E. (2013). Automatic fault detection in grid connected PV systems.
- 531 [6] Dhimish, M., Holmes, V., Mehrdadi, B., & Dales, M. (2017). Simultaneous Fault Detection Algorithm for



- 532 Grid-Connected Photovoltaic Plants. *IET Renewable Power Generation*.
- 533 [7] Chine, W., Mellit, A., Pavan, A. M., & Kalogirou, S. A. (2014). Fault detection method for grid-connected  
534 photovoltaic plants. *Renewable Energy*, 66, 99-110.
- 535 [8] Silvestre, S., da Silva, M. A., Chouder, A., Guasch, D., & Karatepe, E. (2014). New procedure for fault  
536 detection in grid connected PV systems based on the evaluation of current and voltage indicators. *Energy*  
537 *Conversion and Management*, 86, 241-249.
- 538 [9] Dhimish, M., Holmes, V., & Dales, M. (2017). Parallel fault detection algorithm for grid-connected  
539 photovoltaic plants. *Renewable Energy*, 113, 94-111.
- 540 [10] Kim, K. A., Seo, G. S., Cho, B. H., & Krein, P. T. (2016). Photovoltaic hot-spot detection for solar panel  
541 substrings using ac parameter characterization. *IEEE Transactions on Power Electronics*, 31(2), 1121-1130.
- 542 [11] Obi, M., & Bass, R. (2016). Trends and challenges of grid-connected photovoltaic systems—A review.  
543 *Renewable and Sustainable Energy Reviews*, 58, 1082-1094.
- 544 [12] Dhimish, M., Holmes, V., Mehrdadi, B., Dales, M., Chong, B., & Zhang, L. (2017). Seven indicators  
545 variations for multiple PV array configurations under partial shading and faulty PV conditions. *Renewable*  
546 *Energy*.
- 547 [13] Khamis, A., Shareef, H., Bizkevelci, E., & Khatib, T. (2013). A review of islanding detection techniques  
548 for renewable distributed generation systems. *Renewable and Sustainable Energy Reviews*, 28, 483-493.
- 549 [14] Dhimish, M., Holmes, V., Mehrdadi, B., & Dales, M. (2017). The Impact of Cracks on Photovoltaic Power  
550 Performance. *Journal of Science: Advanced Materials and Devices*.
- 551 [15] Zhao, Y., Yang, L., Lehman, B., de Palma, J. F., Mosesian, J., & Lyons, R. (2012, February). Decision  
552 tree-based fault detection and classification in solar photovoltaic arrays. In *Applied Power Electronics*  
553 *Conference and Exposition (APEC), 2012 Twenty-Seventh Annual IEEE (pp. 93-99)*. IEEE.
- 554 [16] Jamshidpour, E., Poure, P., & Saadate, S. (2015). Photovoltaic systems reliability improvement by real-  
555 time FPGA-based switch failure diagnosis and fault-tolerant DC–DC converter. *IEEE Transactions on*  
556 *Industrial Electronics*, 62(11), 7247-7255.
- 557 [17] Chong, B. V. P., & Zhang, L. (2013). Controller design for integrated PV–converter modules under partial  
558 shading conditions. *Solar Energy*, 92, 123-138.
- 559 [18] Boukenoui, R., Salhi, H., Bradai, R., & Mellit, A. (2016). A new intelligent MPPT method for stand-alone  
560 photovoltaic systems operating under fast transient variations of shading patterns. *Solar Energy*, 124, 124-  
561 142.
- 562 [19] Mutlag, A. H., Shareef, H., Mohamed, A., Hannan, M. A., & Abd Ali, J. (2014). An improved fuzzy logic  
563 controller design for PV inverters utilizing differential search optimization. *International Journal of*  
564 *Photoenergy*, 2014.
- 565 [20] Sa-ngawong, N., & Ngamroo, I. (2015). Intelligent photovoltaic farms for robust frequency stabilization in  
566 multi-area interconnected power system based on PSO-based optimal Sugeno fuzzy logic control.  
567 *Renewable Energy*, 74, 555-567.
- 568 [21] Palaniswamy, A. M., & Srinivasan, K. (2016). Takagi-Sugeno fuzzy approach for power optimization in  
569 standalone photovoltaic systems. *Solar Energy*, 139, 213-220.
- 570 [22] Dhimish, M., Holmes, V., Mehrdadi, B., & Dales, M. (2017). Diagnostic method for photovoltaic systems  
571 based on six layer detection algorithm. *Electric Power Systems Research*, 151, 26-39.

- 572 [23] Dhimish, M., Holmes, V., Mehrdadi, B., & Dales, M. (2017). Multi-Layer Photovoltaic Fault Detection  
573 Algorithm. *High Voltage*.
- 574 [24] Yagi, Y., Kishi, H., Hagihara, R., Tanaka, T., Kozuma, S., Ishida, T., ... & Kiyama, S. (2003). Diagnostic  
575 technology and an expert system for photovoltaic systems using the learning method. *Solar energy*  
576 *materials and solar cells*, 75(3), 655-663.
- 577 [25] Chine, W., Mellit, A., Lughfi, V., Malek, A., Sulligoi, G., & Pavan, A. M. (2016). A novel fault diagnosis  
578 technique for photovoltaic systems based on artificial neural networks. *Renewable Energy*, 90, 501-512.
- 579 [26] Mellit, A., Sağlam, S., & Kalogirou, S. A. (2013). Artificial neural network-based model for estimating the  
580 produced power of a photovoltaic module. *Renewable Energy*, 60, 71-78.
- 581 [27] Polo, F. A. O., Bermejo, J. F., Fernández, J. F. G., & Márquez, A. C. (2015). Failure mode prediction and  
582 energy forecasting of PV plants to assist dynamic maintenance tasks by ANN based models. *Renewable*  
583 *Energy*, 81, 227-238.
- 584 [28] Sepasi, S., Reihani, E., Howlader, A. M., Roose, L. R., & Matsuura, M. M. (2017). Very short term load  
585 forecasting of a distribution system with high PV penetration. *Renewable Energy*.
- 586 [29] McEvoy, A., Castaner, L., Markvart, T., 2012. *Solar Cells: Materials, Manufacture and Operation*.  
587 Academic Press.
- 588 [30] Sera, D., Teodorescu, R., & Rodriguez, P. (2007). PV panel model based on datasheet values. Paper  
589 presented at the 2392-2396. doi:10.1109/ISIE.2007.4374981
- 590 [31] Dhimish, M., Holmes, V., Dales, M., & Mehrdadi, B. (2017). The effect of micro cracks on photovoltaic  
591 output power: case study based on real time long term data measurements. *Micro & Nano Letters*.
- 592 [32] Dhimish, M., Holmes, V., Dales, M., Mather, P., Sibley, M., Chong, B., & Zhang, L. (2017, June). Fault  
593 detection algorithm for multiple GCPV array configurations. In *PowerTech, 2017 IEEE Manchester* (pp. 1-  
594 6). IEEE.
- 595 [33] Huang, C., Bensoussan, A., Edesess, M., & Tsui, K. L. (2016). Improvement in artificial neural network-  
596 based estimation of grid connected photovoltaic power output. *Renewable Energy*, 97, 838-848.
- 597 [34] Amrouche, B., & Le Pivert, X. (2014). Artificial neural network based daily local forecasting for global  
598 solar radiation. *Applied energy*, 130, 333-341.
- 599 [35] Cervone, G., Clemente-Harding, L., Alessandrini, S., & Delle Monache, L. (2017). Short-term photovoltaic  
600 power forecasting using Artificial Neural Networks and an Analog Ensemble. *Renewable Energy*, 108,  
601 274-286.
- 602 [36] Etemadi, A. (2016). Fault Detection for Photovoltaic Systems Based on Multi-resolution Signal  
603 Decomposition and Fuzzy Inference Systems. *IEEE Transactions on Smart Grid*.
- 604 [37] Dhimish, M., Holmes, V., Mehrdadi, B., Dales, M., & Mather, P. (2018). Photovoltaic fault detection  
605 algorithm based on theoretical curves modelling and fuzzy classification system. *Energy*,  
606 doi.org/10.1016/j.energy.2017.08.102.

**Highlights:**

- PV fault detection algorithm based on the analysis of the voltage and the power is presented.
- Two machine learning techniques were developed and compared briefly.
- Four different Artificial neural networks (ANN) are used for detecting PV faults.
- Two fuzzy logic systems (Mamdani & Sugeno) are used for examining faults in PV systems.